“Cold-Flow” Experiments Supporting CFD of Mixing Flowfields for High-Speed Fuel Injectors for Scramjet Applications

Tomasz G. Drozda

Hypersonic Airbreathing Propulsion Branch, NASA Langley Research Center

UT Austin

March 24, 2022

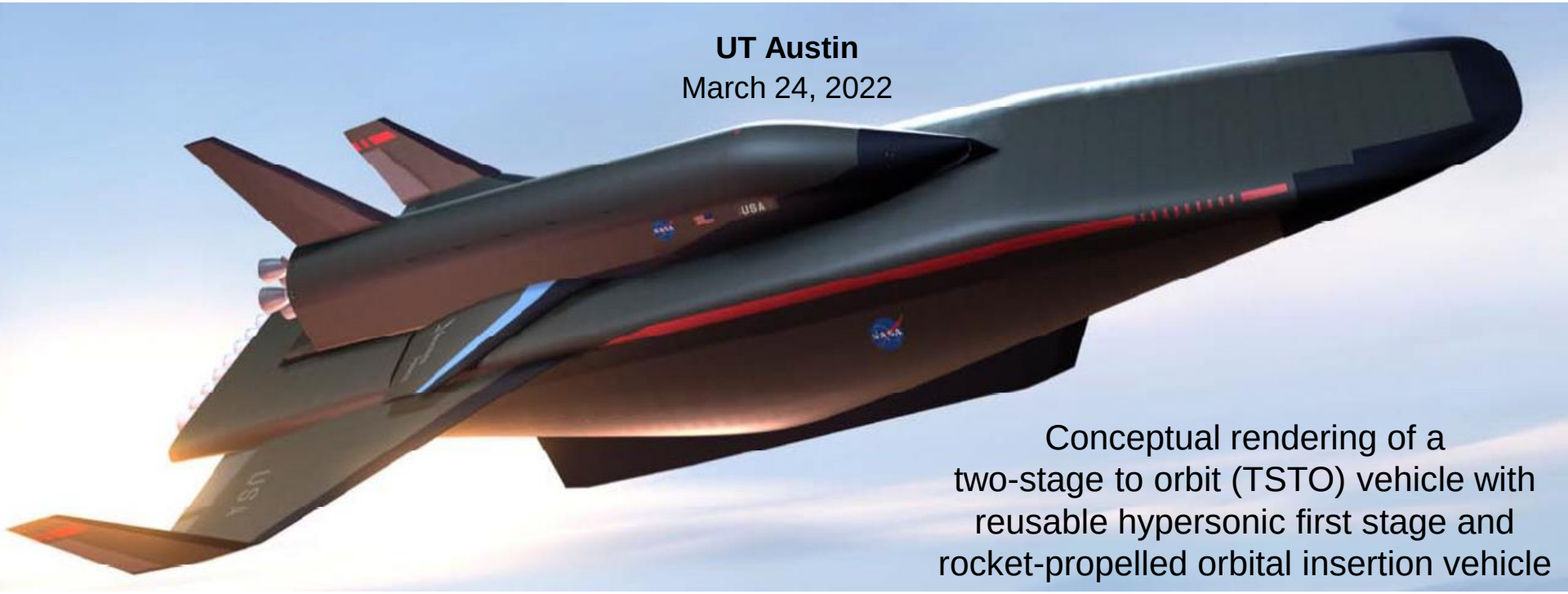

Conceptual rendering of a two-stage to orbit (TSTO) vehicle with reusable hypersonic first stage and rocket-propelled orbital insertion vehicle

Acknowledgements:

Karen Cabell, Cody Ground, Neal Hass, Robert Baurle
Hypersonic Airbreathing Propulsion Branch, NASA Langley Research Center

Paul Danehy, Jennifer Inman, Ross Burns, Brett Bathel, Steve Jones
Advanced Measurement and Data Systems Branch, NASA Langley Research

Austin Ziltz
Calspan

Rajiv Shenoy, Jake Lampenfield, Brad Passe
Analytical Mechanics Associates, Inc.

Rohan Deshmukh, Walker Knapp
NASA LaRC Summer Interns

Outline

Part I: Overview

- Introduction to Air Breathing Engines
- Ramjets/Scramjets vs. Gas Turbines
- Schematic of Scramjet Propulsion System
- Hypersonic Access-to-Space
- Thrust and Mass Flow Rate Through the Engine
- Aerothermodynamic Heating
- Ground Experimentation for High-Speed Flows
- Hypersonic Propulsion as an Aeroscience
- Advantaged, Disadvantages, and Challenges

Part II: Details

- Efficient Fuel Injection and Mixing for Scramjets
- Enhanced Injection and Mixing Project at NASA Langley
- Simulations of Mixing Flow Fields
- Planar Laser Induced Fluorescence (PLIF) for Flow Visualizations
- In-steam Gas Sampling
- Summary and Conclusions

Introduction: Air-breathing Engines

Air-breathing Engines

- Internal Combustion Engine
- Turboprop
- Turbofan
- Turbojet
- Ramjet (RJ)
- Scramjet (SJ)
- Turbine-based combined cycle (TBCC)
- Rocket-based combined cycle (RBCC)
- Air-augmented or ducted rocket (DR)
- Pulse detonation engine (PDE)
- Rotating detonation engine (RDE)

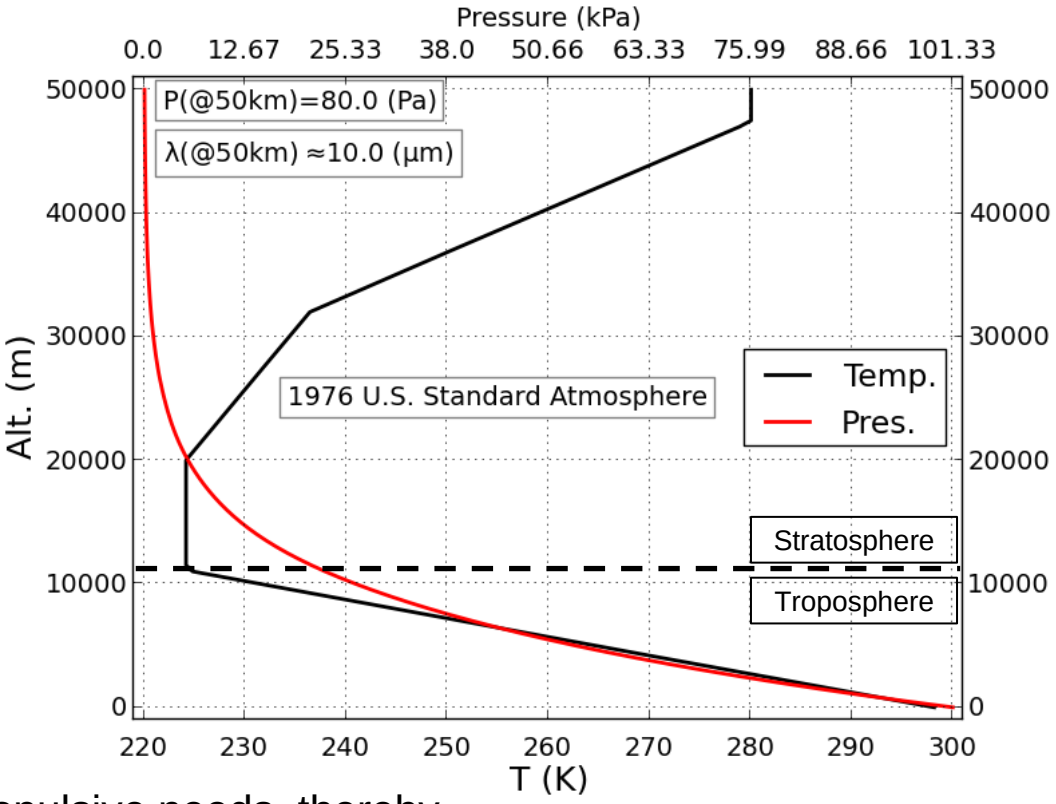

Main benefit:

- Vehicle only needs to carry fuel for its propulsive needs, thereby
  - allowing for larger payloads or …
  - lighter vehicle (less structure to support weight) or …
  - more fuel for longer range

- Not trivial because for hydrocarbon fuels, oxidizer represents about 94% of total propellant mass (fuel+oxidizer).
- Rocket-powered airliner would be about 7.5x heavier at TO with propellant to max. TO weight ratio of about 93%. (assuming airliner with fuel/(max. TO wt.) ratio of 40% and no change in vehicle dry weight)

Ramjet/Scramjet vs. Turbo Propulsion

Conventional
Gas Turbine Engine
(Subsonic to Low-Supersonic)

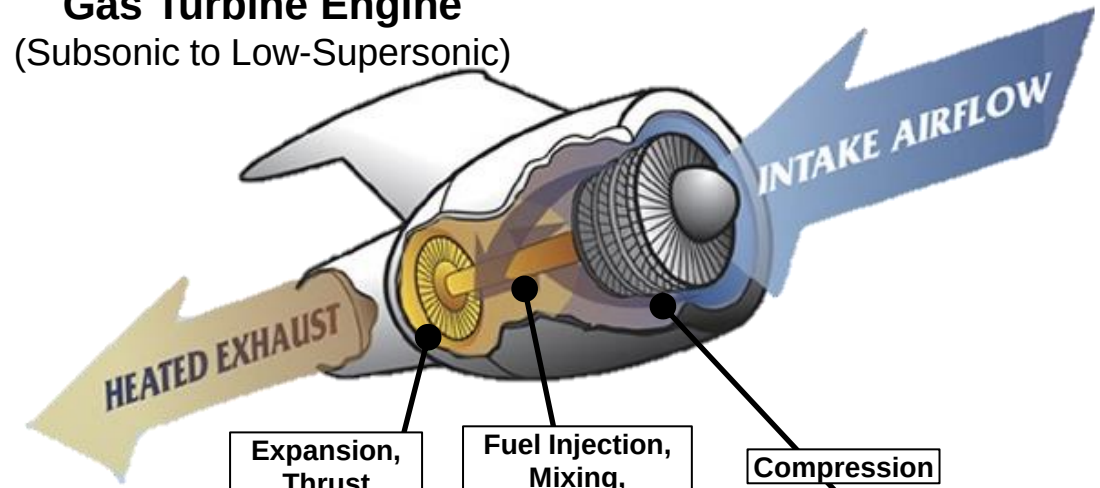

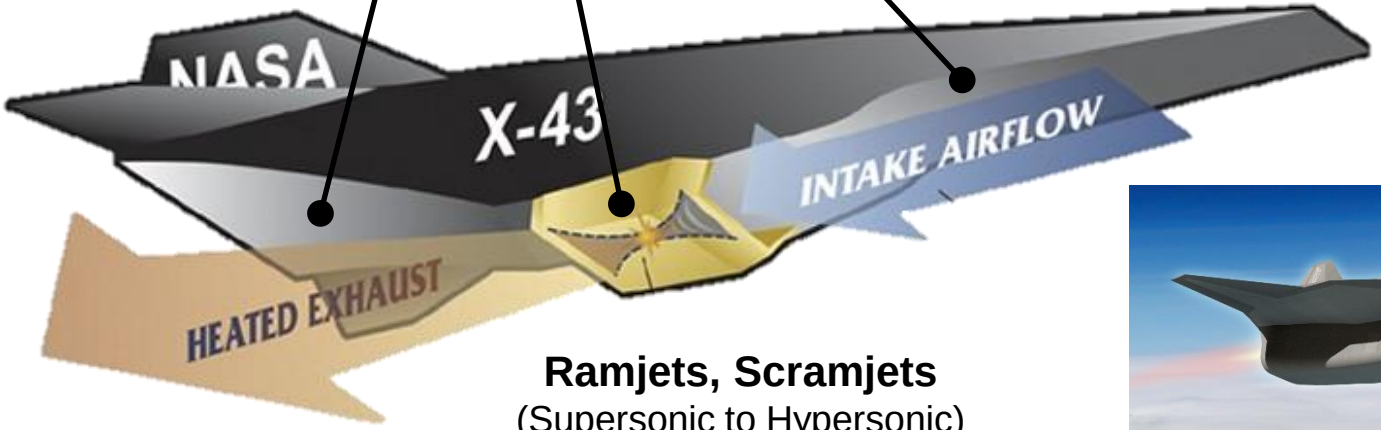

Ramjets, Scramjets
(Supersonic to Hypersonic)

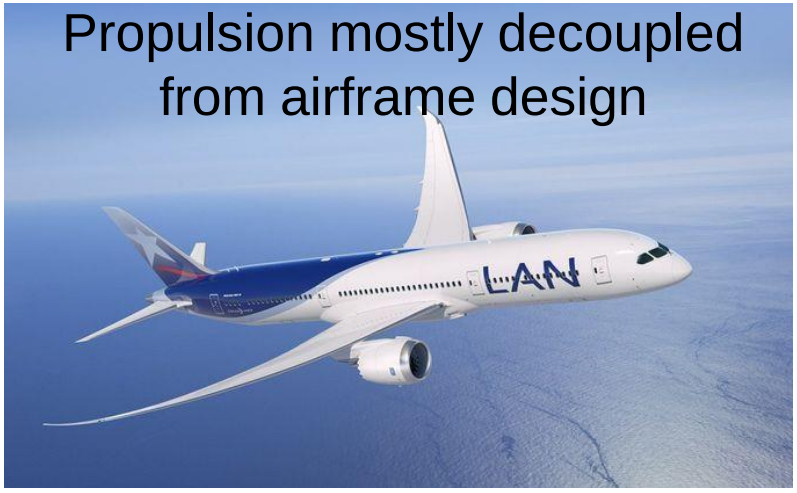

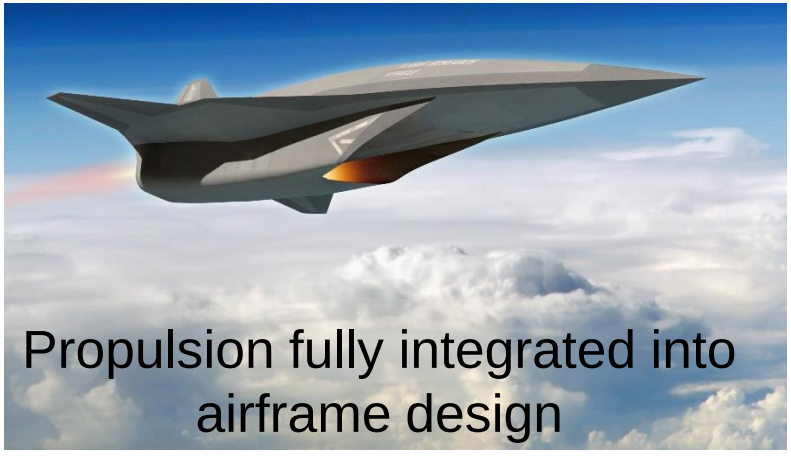

Gas turbines and ramjet/scramjet both qualitatively operate on a Brayton* thermodynamic cycle

Scramjet Propulsion System

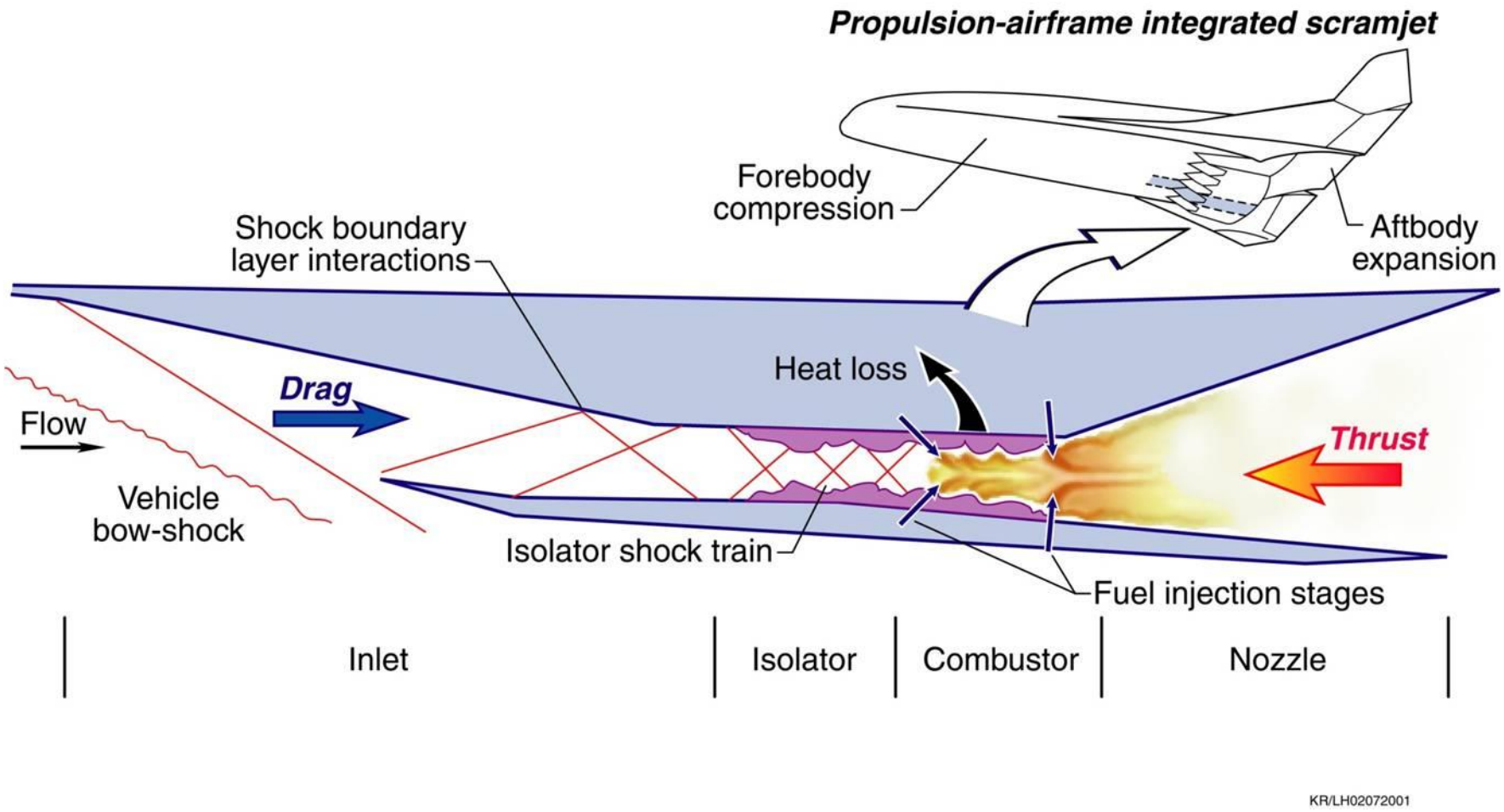

Heiser, W. H. and Pratt, D. T. "**Hypersonic Airbreathing Propulsion**" AIAA Education Series,1994

Hypersonic Access-to-Space Flight Trajectories

- Bernoulli's equation for a moving fluid gives rise to the *Dynamic Pressure*:

$$q_0(Pa) = \frac{\rho u^2}{2} = \frac{1}{2}\gamma p M_0^2$$

which is the kinetic component of the total pressure

- *q* is a useful aerodynamic parameter that is related to lift and drag forces of a vehicle:

$$L(N) = q_0\, C_L\, S$$
$$D(N) = q_0\, C_D\, S$$

- *When q* is too large, the structural forces and the drag can become excessive.
- When *q* is too small, the wing area required for controlled sustained flight may become too large

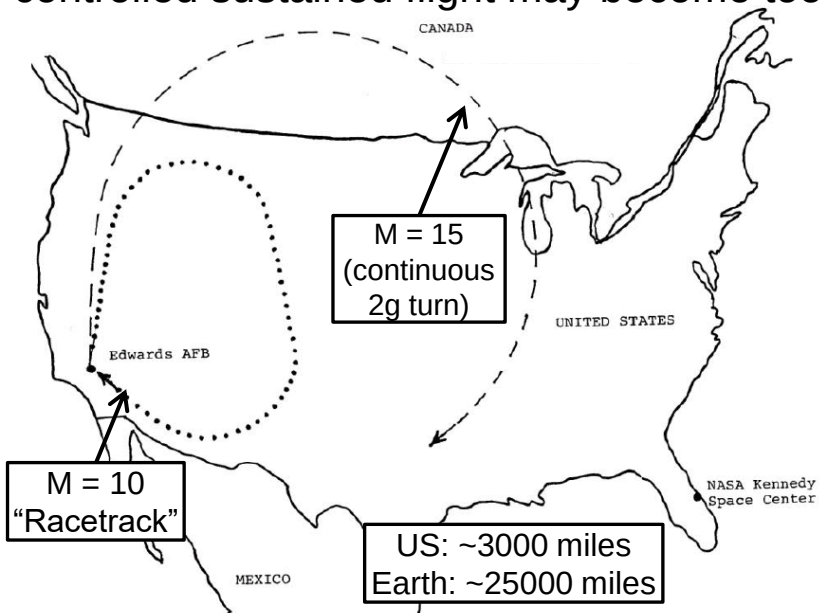

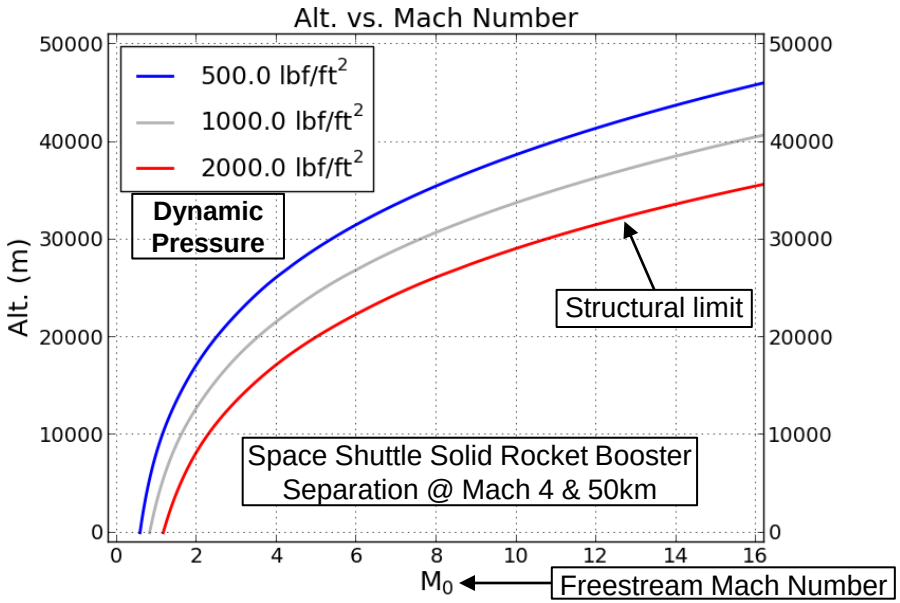

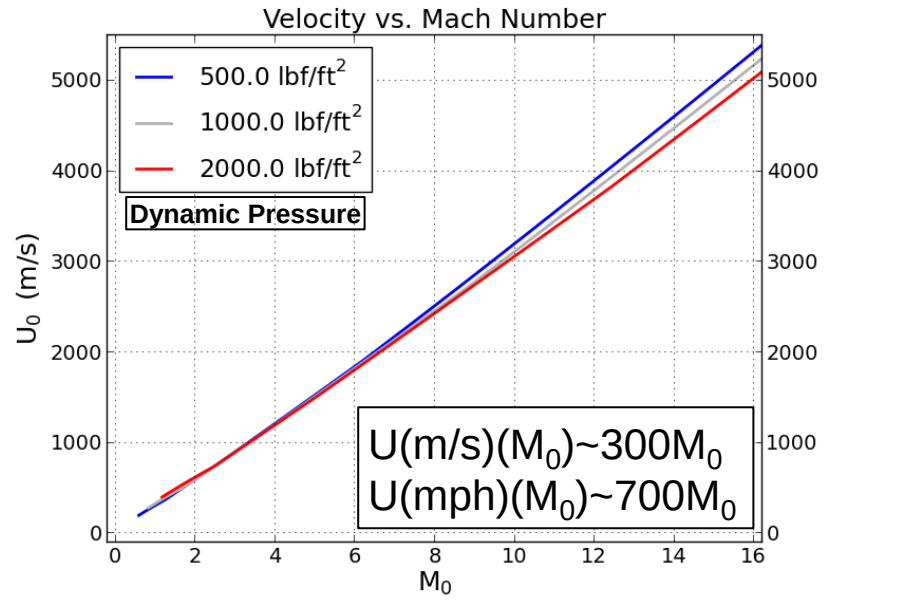

Mass Flow Rate and Engine Thrust

- Mass flow rate of air through the engine can also be related to the *Dynamic Pressure, q*:

$$\dot{m}_0 \left(\frac{kg}{s}\right) = \dot{m_0}'' A_0 = \frac{2q}{u_0} A_0$$

- And since mass flow rate through the engine is related to engine net thrust (obtained from the *conservation of momentum*), we obtain:

$$F(N) = (p_e - p_0)A_e + \frac{2q}{u_0} A_0 (u_e(1+f) - u_0)$$

- *Specific Impulse (Isp)* is a measure of how efficiently a vehicle uses its propellant to generate thrust:

$$I_{sp}(s) = \frac{F}{g\,\dot{m}_0\,f}$$

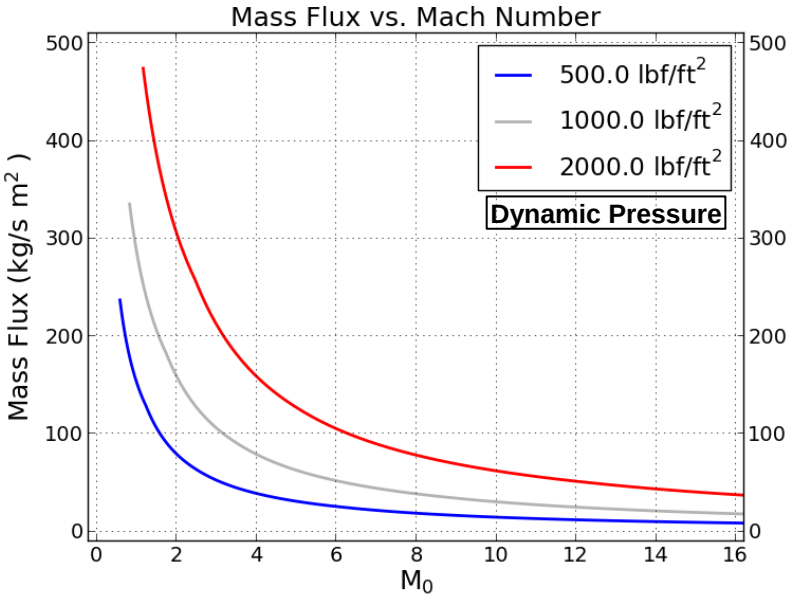

- One of the most important non-dimensional parameters is the *Reynolds Number*:

$$Re = \frac{2\,q_0\,L}{u_0\,\mu_0}, \qquad Natural\ Transition\ for\ Re > 10^7$$

- *Re* indicates to the designer whether the boundary layers are laminar, transitional, or turbulent
  - Externally, *laminar boundary layers* are preferred due to lower skin friction and wall heat transfer
  - Internally, *turbulent boundary layers* are preferred due to greater resistance to flow separation

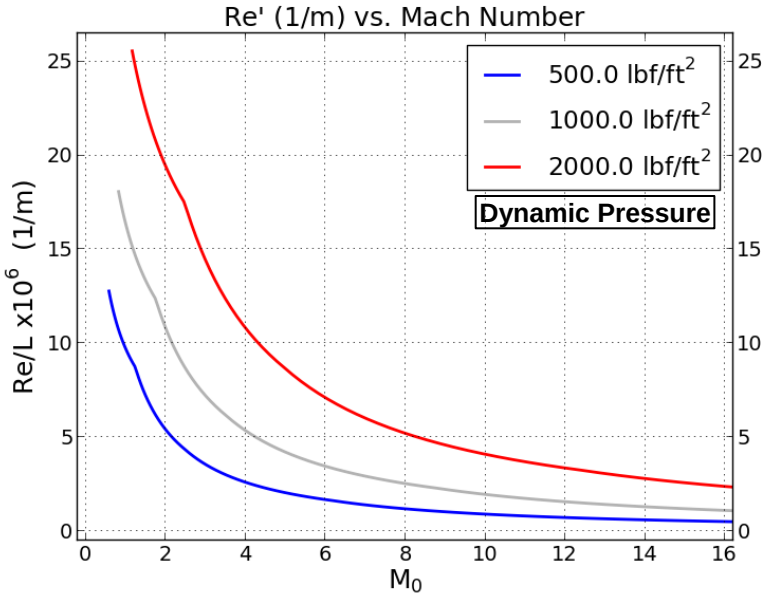

Aero-Thermodynamic Heating

- From the definition of total energy and static enthalpy, we have:

$$e^t = e + k = h - \frac{p}{\rho} + k = h^t - \frac{p}{\rho},$$

$$h = \sum_{\alpha} Y_{\alpha} \int_0^T dT' Cp_{\alpha}(T')$$

- If we stagnate the flow such that all of *k* is absorbed into the *h*, then the flow's temperature must rise. This new temperature of the stagnated flow is called *stagnation or total temperature*.
  - In subsonic flows, the kinetic energy is small, and so the static and total temperatures are about the same
  - In supersonic flows, the kinetic energy is large, and the ratio of static and total temperatures depends on the Mach number:

$$\frac{T_t}{T} = \left(1 + \frac{k}{h}\right) = \left(1 + \frac{\gamma - 1}{2} M^2\right)$$

  - In hypersonic flows, the kinetic energy is >> than the static enthalpy such that most of the flow's energy is in the kinetic form, e.g., at Mach 7, the kinetic energy is an order of magnitude larger than the enthalpy.
- Heating (and cooling) considerations drive material selection in high-speed applications.

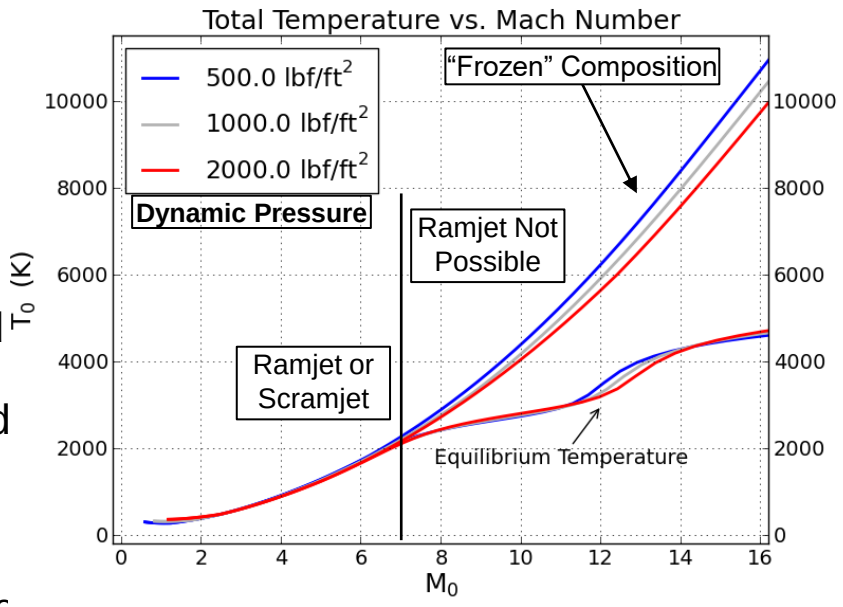

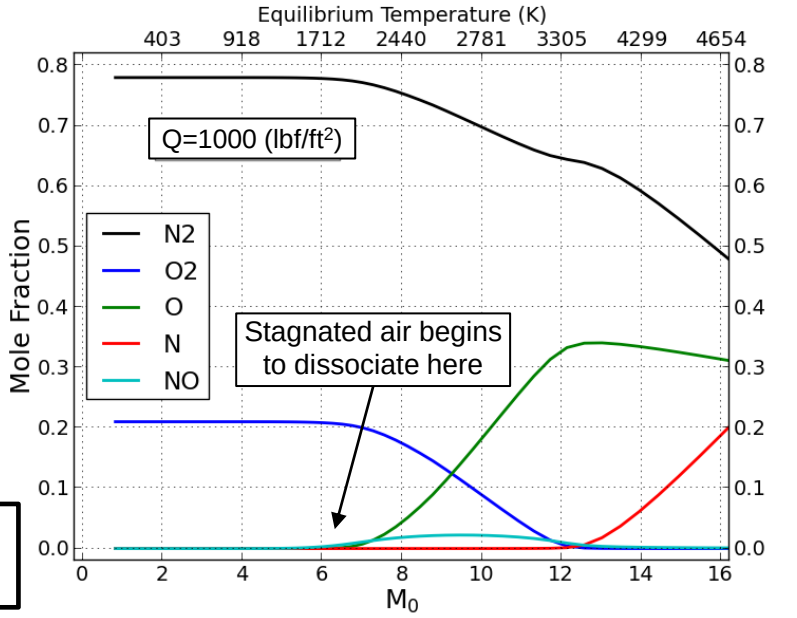

Note that at a moderate Mach number of 3.5 (SR-71) the vehicle skin temperature reaches 500-600°F during flight

Ground Experiments for High-Speed Propulsion

Flight

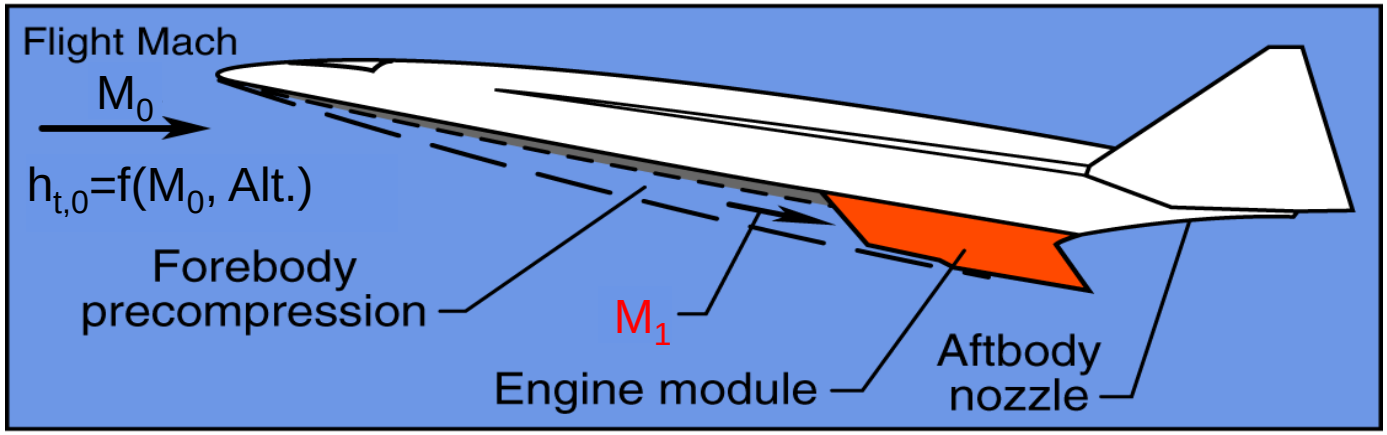

Simulation in ground facility

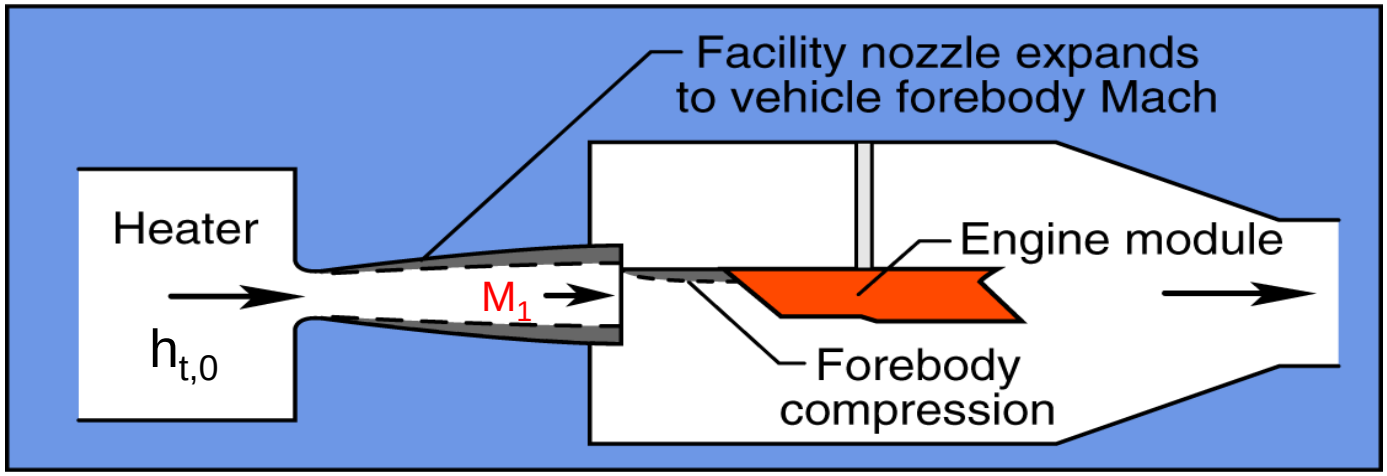

Hypersonic Propulsion as an Aeroscience

M&S ($)
100s/year

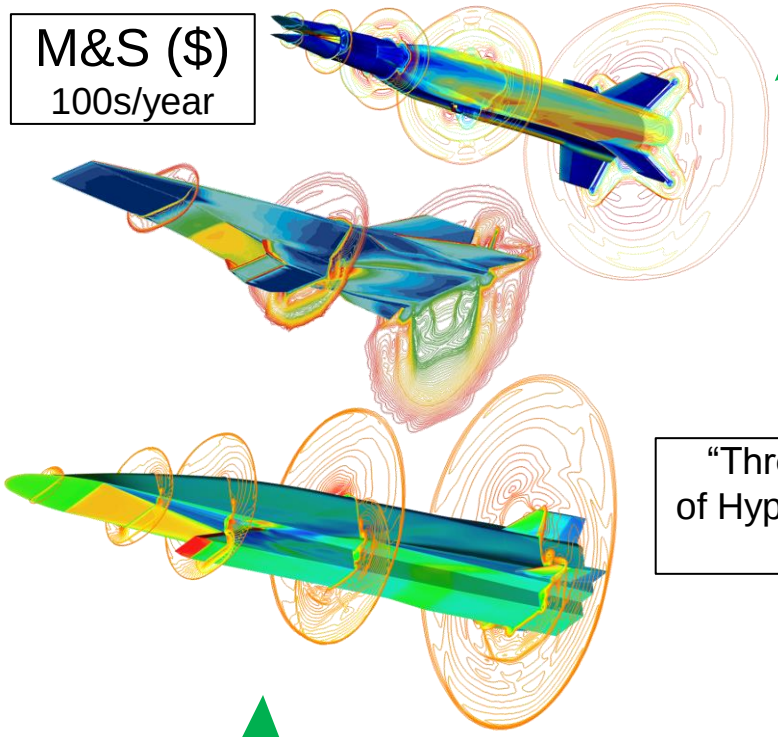

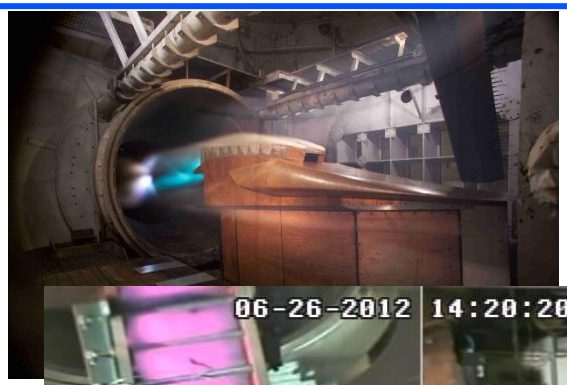

Ground Testing ($$$)
10/year

"Three Legged Stool" of Hypersonic Propulsion Aeroscience

Flight Testing ($$$$$$)
1/year

Advantages, Disadvantages, and Challenges

Advantages:

+ Higher thrust efficiency
+ Fewer moving parts
+ Increased launch abort options
+ Horizontal launch and landing
+ Increased reusability
+ Lower operational cost (expected)

Disadvantages:

– No static thrust (“boost” needed)
– No power for subsystems (need batteries, fuel cells, APUs?)
– Active cooling is required and/or
– Need yet-to-be developed advanced high temperature materials

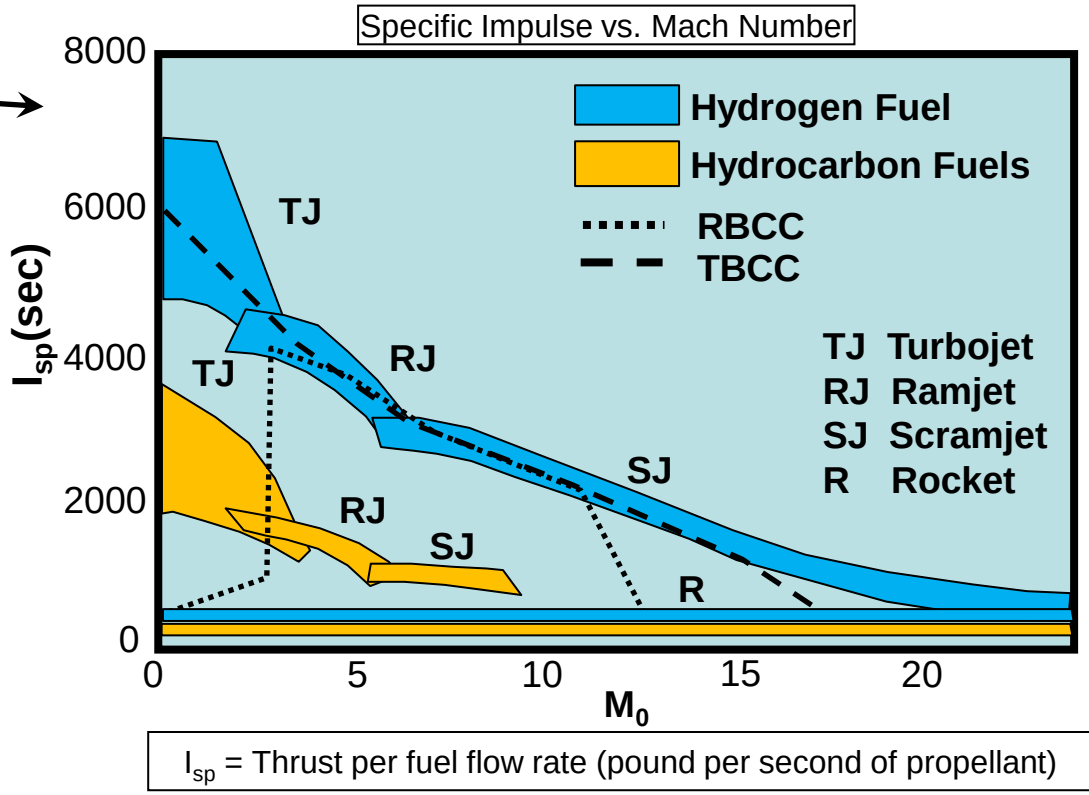

I_{sp} = Thrust per fuel flow rate (pound per second of propellant)

Challenges:

- Fully integrated vehicle airframe and engine (challenging to design and analyze performance)
- Ground and flight tests are difficult to execute and are expensive
- Robust operation over a wide range of Mach numbers (actuated flowpath doors, e.g. SR-71)
  - Decreasing air density with altitude (engine capture area must increase to maintain thrust)
  - Performance of high-speed inlets and nozzles
- Structural integrity vs. weight for flight at high dynamic pressures (to capture more air mass)
- Small flow residence time in the combustor (need efficient fuel-air mixing and combustion)

Efficient Fuel Injection and Mixing for Scramjets

- Optimized high-speed fuel injectors are needed for Scramjet engines that will propel the next generation of vehicles for access to space and hypersonic civil transport
- Enhanced Injection and Mixing Project (EIMP) at NASA Langley is investigating the physics of fuel injection & mixing for high-speed flight applications
  - Objectives:
    - increase knowledge and understanding of the fundamental physics governing fuel-air mixing
    - develop strategies for improving injector performance
    - develop the functional relationships between mixing efficiency, losses and flowpath geometry
  - Approach: combined experimental/numerical
- Nitric Oxide Planar Laser Induced Fluorescence (NO PLIF) is being used for flow visualization in fuel-air mixing experiments for the EIMP
- To compare the PLIF images with the CFD, a LIF model (LIFQWIK) is developed and applied to the results of the CFD simulations to obtain computationally-equivalent PLIF images. (Computational Flow Imaging, or CFI)
- PLIF and CFI (CFD+LIFQWIK) have been synergistic in the current experiments:
  - PLIF identifying areas where CFD needed improvement
  - CFI identifying experimental errors and limitations that could be addressed in the future
- Because PLIF proves to be qualitative, in-stream gas sampling is currently being conducted to obtain quantitative mixing data via surrogate mixing metrics

Part II summarizes the practical deployment and use of experiments to establish a level of confidence in the CFD for the high-speed mixing simulations in scramjets

Enhanced Injection and Mixing Project

- **Experiments in Langley Arc-Heated Scramjet Test Facility (AHSTF)**
  - Helium injection into Mach 6 airflow
  - Cold flow: T_t=728-978K (1310 to 1760°R)
  - Injectors mounted on open flat plate

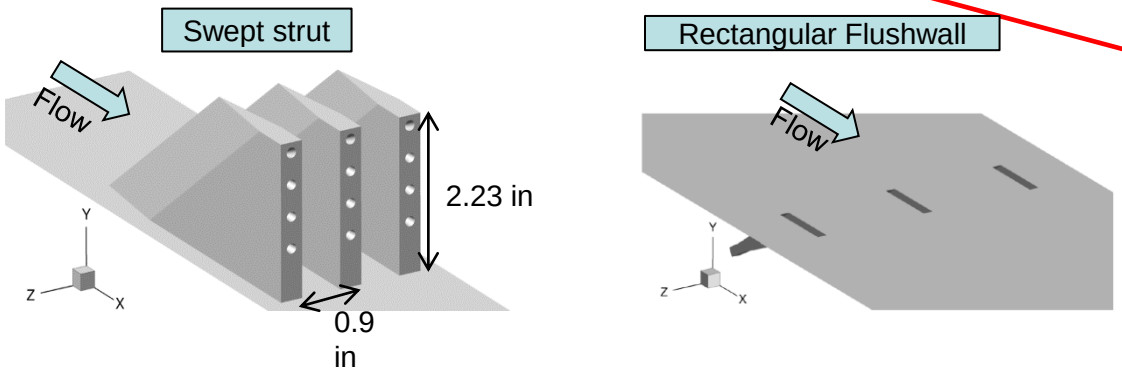

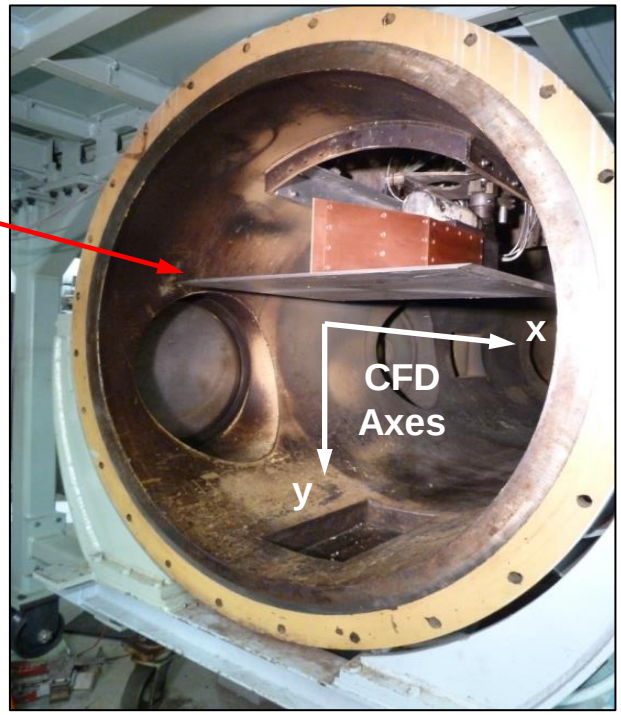

  - Flow visualization via Nitric Oxide Planar Laser Induced Fluorescence (NO PLIF)
  - Quantitative measurements via in-stream probes
    - Gas sampling (helium mole fraction)
    - Pitot pressure
    - Total temperature

- **CFD (using VULCAN-CFD)**
  - Reynolds-averaged simulations (RAS) calibrated with experimental data
  - Large eddy simulations (LES) to be used for select cases
  - Needed to calculate mixing performance (mixing efficiency and total pressure recovery)

CFD Simulations for CFI

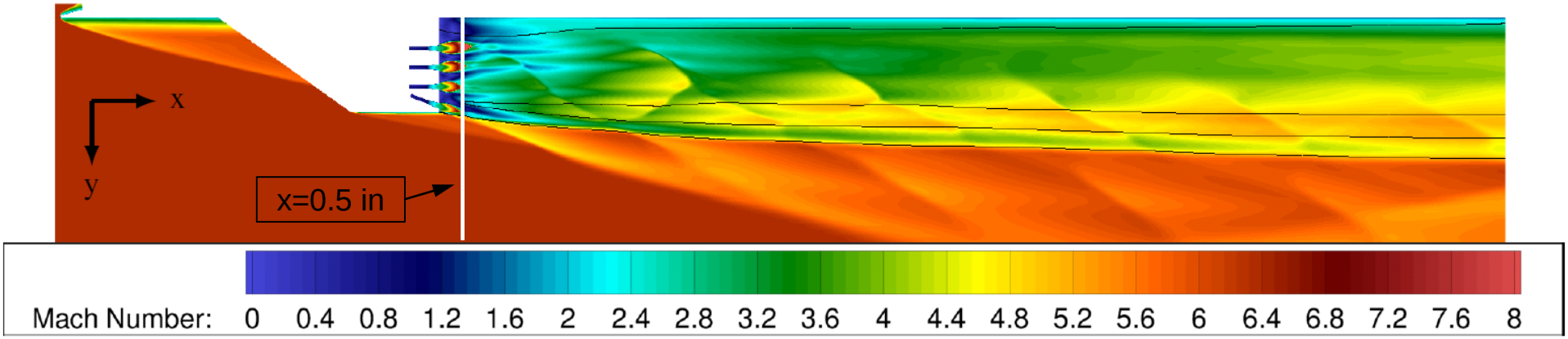

- RAS and LES obtained using VULCAN-CFD
- Black isocontour lines denote mass fraction of 0.0285 (stoichiometry of hydrogen)
- Helium is still mostly confined to areas just downstream of the injector bodies (injection near field)

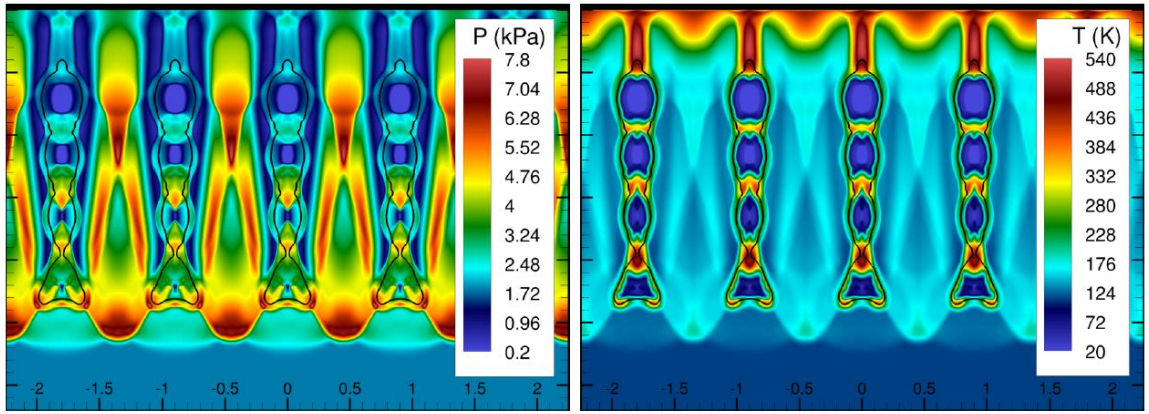

Contours of pressure, and temperature from the laser plane at 0.5 inches downstream from the injector

LIF model is required to directly compare the CFD to PLIF

Sensitivity to the Turbulence Model

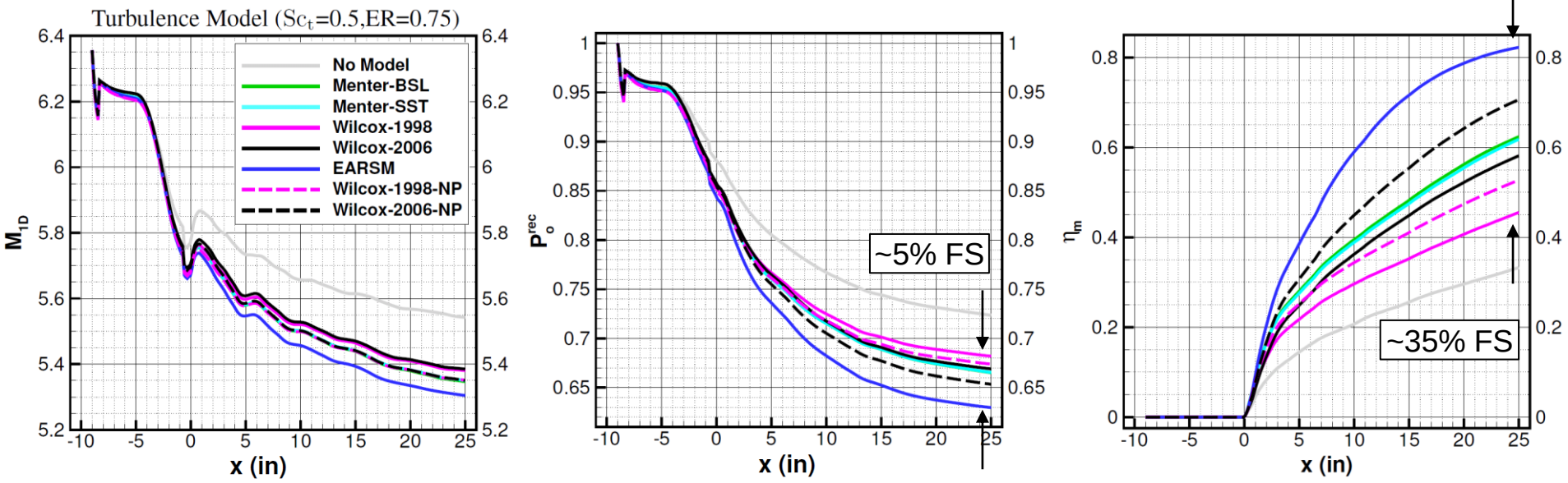

- Simulation without a turbulence model produces the least amount of losses and mixing because it lacks the turbulence model contribution to the scalar diffusion.
- The largest mixing is induced by the EARSM model (this model produces the largest values of the eddy viscosity at the fuel-air interface for the current cases).
- Choice of the turbulence model has a modest influence on the Mach number and total pressure recovery, and fairly significant influence on the mixing efficiency (comparable to the effect of varying the ER from 0.375 to 1.5)
- Menter-BSL and Menter-SST models lie about midway of the group, hence these models could offer a practitioner a greater access to the solution space when calibrating with the experimental data.

All the models utilized in the present study are routinely used by RAS practitioners in the field

Sensitivity to the Turbulent Schmidt Number

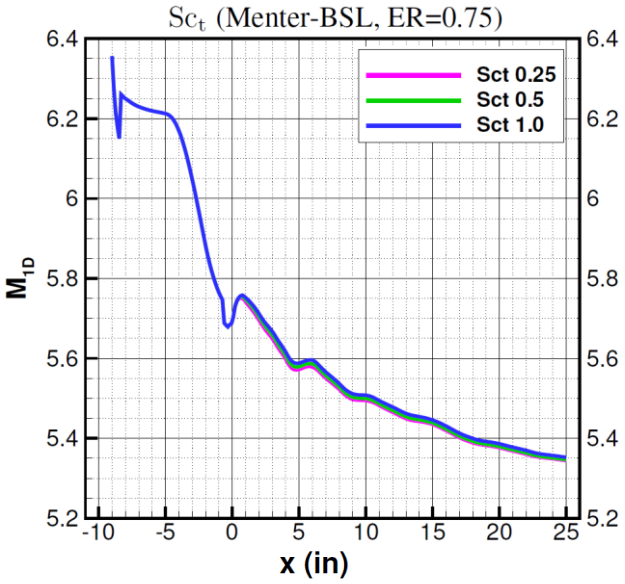

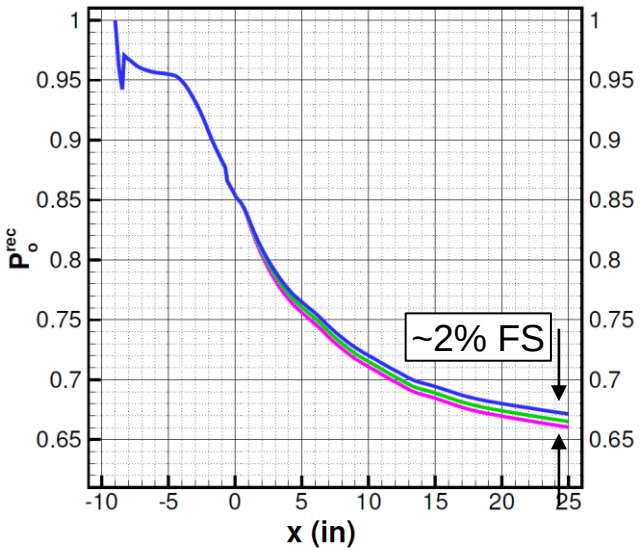

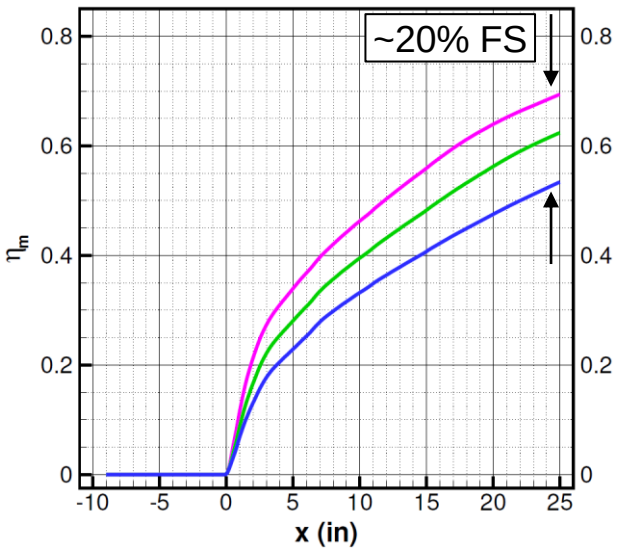

- Typical Favre-averaged transport equation solved by RAS for mixing and reacting species:

$$\frac{\partial \overline{\rho}\widetilde{Y}_\alpha}{\partial t} + \frac{\partial \overline{\rho}\,\widetilde{u}_i \widetilde{Y}_\alpha}{\partial x_i} = \frac{\partial}{\partial x_i}\left(\frac{\mu}{Sc} + \boxed{\frac{\mu_t}{Sc_t}}\right)\frac{\partial \widetilde{Y}_\alpha}{\partial x_i} + \overline{\omega}_\alpha$$

- Turbulent Schmidt number (Sc_t) has a weak influence on both the Mach number and the total pressure recovery.

- Influence on the mixing efficiency is similar to that of the turbulence model.

Results underscore the requirement for robust experimental data, high-fidelity simulations (e.g., DNS, LES), and/or extensive subject matter expertise

Experiments: PLIF

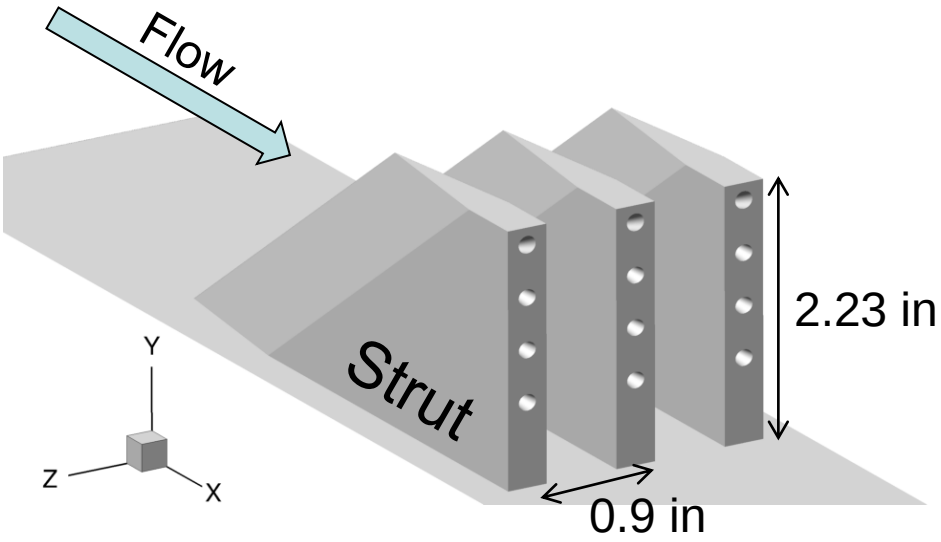

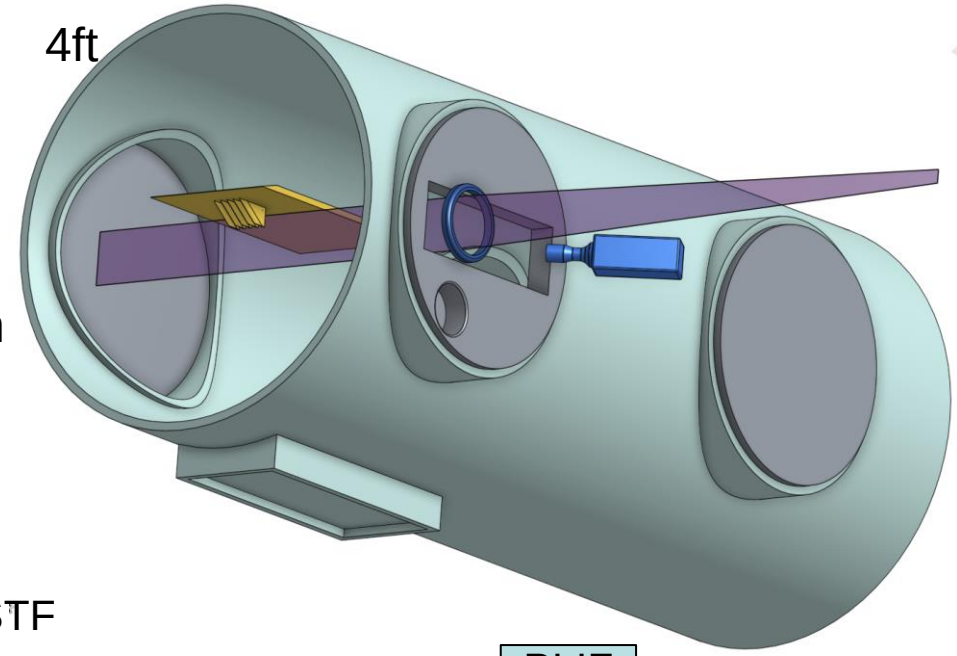

- NO is produced in the arc-heater of the AHSTF
- UV laser beam, formed into a sheet, interrogates either streamwise or cross-stream slices of the flow.
- The UV light excites fluorescence from the NO molecules, which is detected by a CCD camera.
- Since NO is present only in the facility air and not the fuel, the absence of signal indicates pure helium
- Gas cell is used for LIF signal verification
- PLIF images are obtained at 10 Hz

PLIF

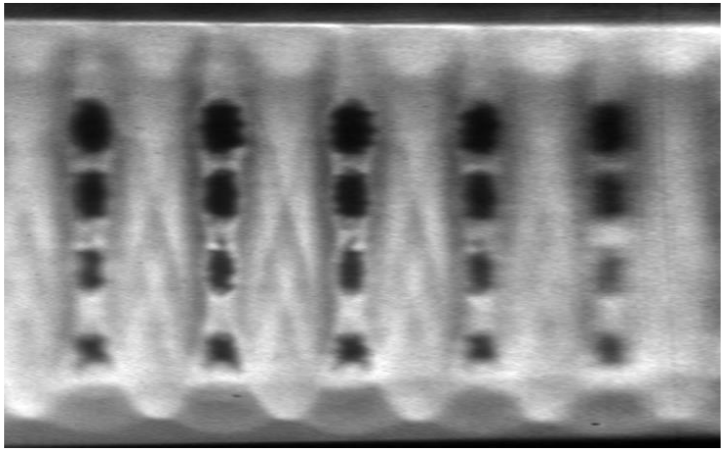

PLIF is used for flow visualization, while gas sampling gives quantitative mixing data

Experiments: PLIF Time Average vs. Instantaneous

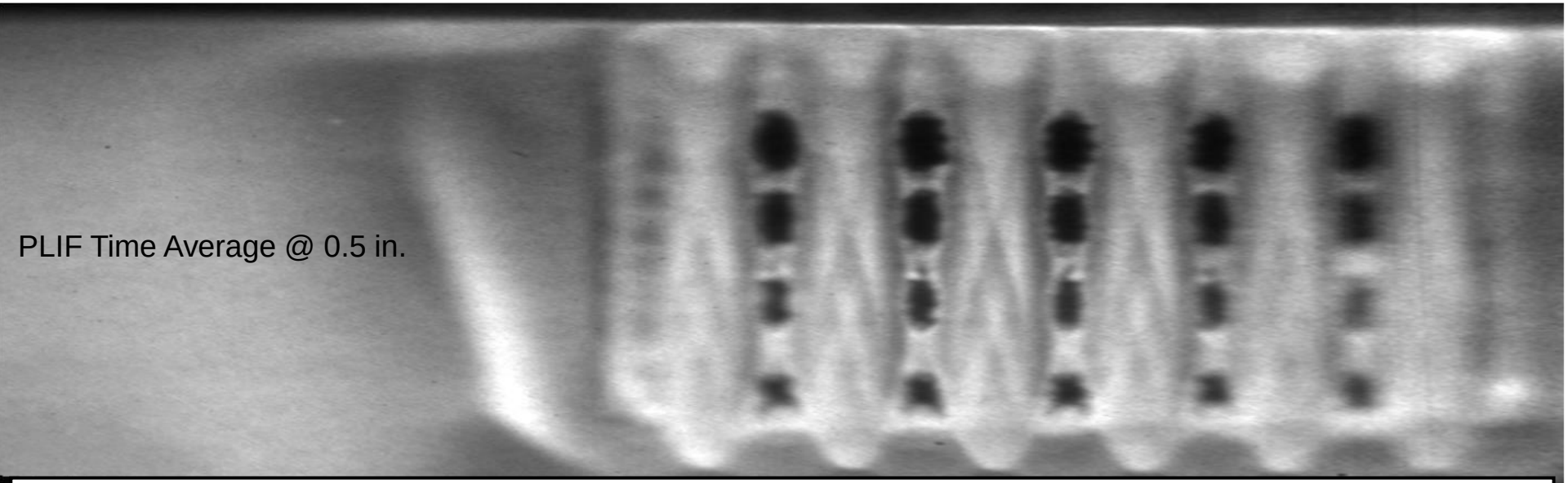

LIF model is required to directly compare the CFD to PLIF

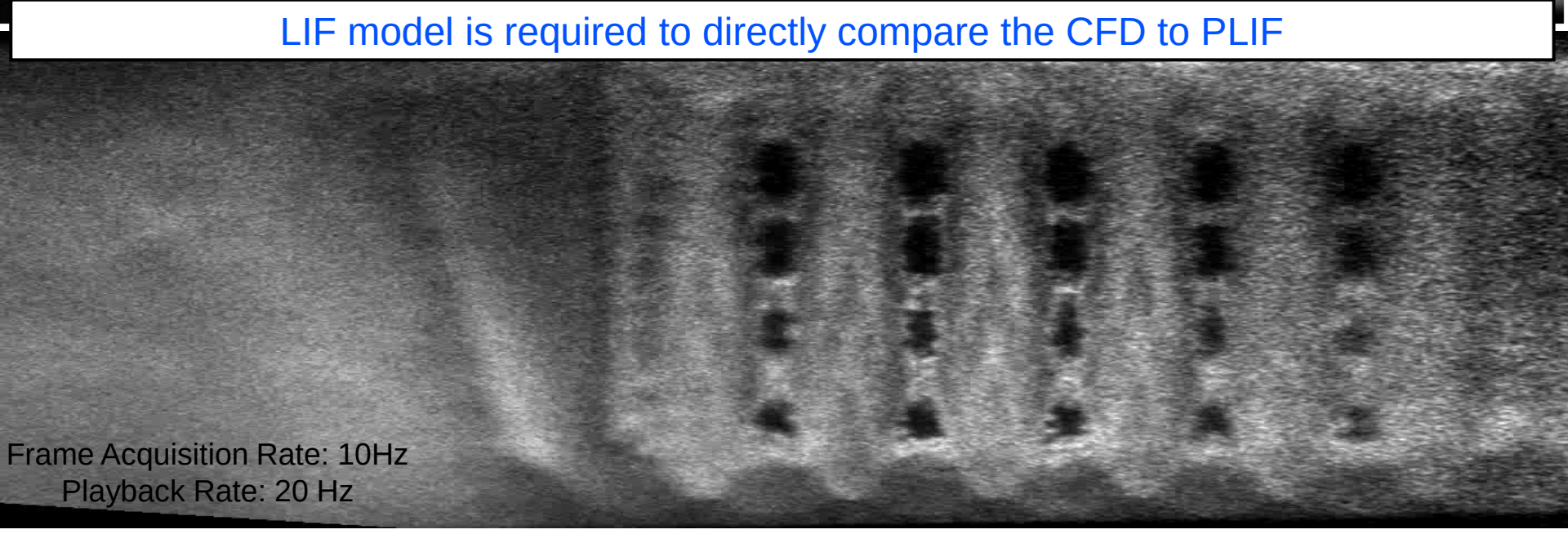

LIF Modeling for CFI (LIFQWIK)

- Modified LIF model of Paul et al. (1993) is used to compute the LIF signal from the CFD data (called LIFQWIK here)
- Similar model was previously also implemented by Ivey et al. (2011)

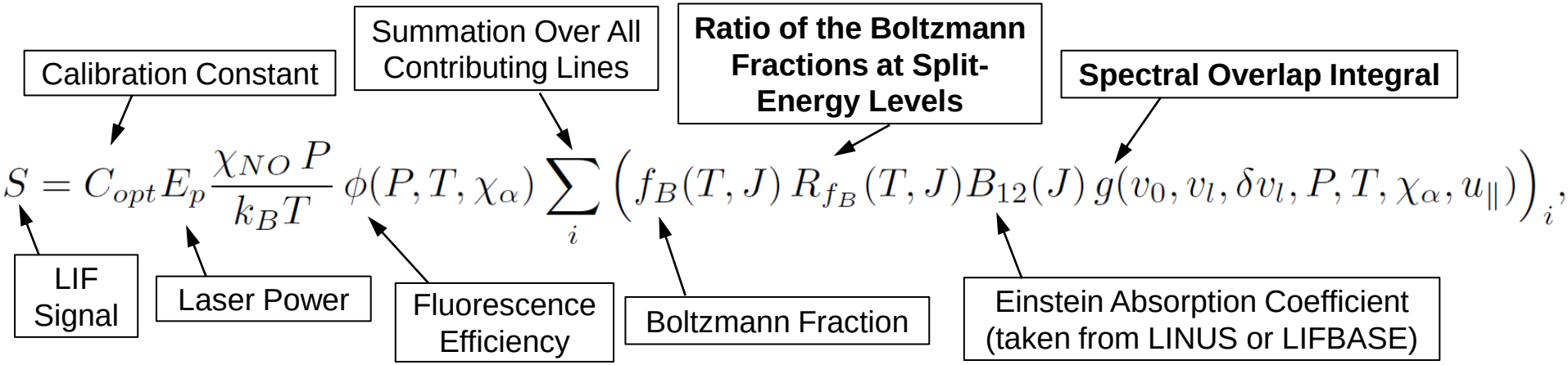

- LIFQWIK
  - is quick to implement and numerically evaluate but needs some inputs from more complete models like LIFBASE or LINUS
  - uses **Voigt profile** to model the spectral overlap integral
  - optionally accounts for the **dual-peaked laser profile** (technical issue identified with the laser)

- LIFBASE is available from SRI International (www.sri.com)
- LINUS was developed at the Australian National University in the late 90s

From here on CFI refers to LIF signal computed from CFD using LIFQWIK

Gas Cell Spectra: LIF Model Verification

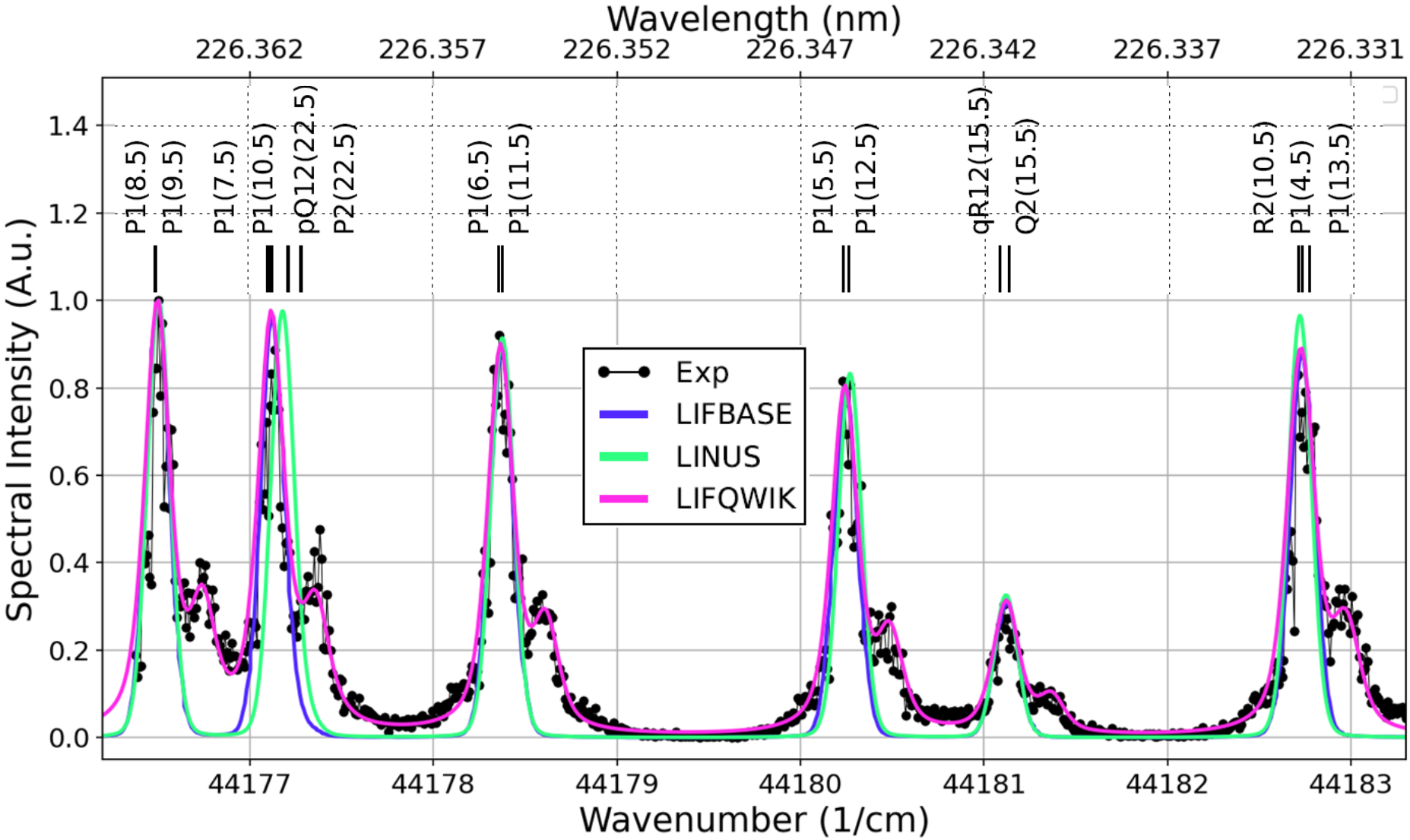

LIF model performs well compared to LIFBASE and LINUS at fraction of cost

PLIF and CFI

- Dark regions indicate fuel (absence of NO)
- The differences observed between the PLIF and CFI are due to:
  - flow unsteadiness (including facility air NO fluctuations),
  - as built geometric differences between adjacent injectors,
  - facility air flow distortion,
  - facility vibration,
  - quality of the experimental optics,
  - optical system resolution (CCD pixel size vs. lp/mm),
  - laser light absorption,
  - laser detuning (Doppler shift),
  - experimental image postprocessing,
  - and errors from turbulence modeling in the CFD.

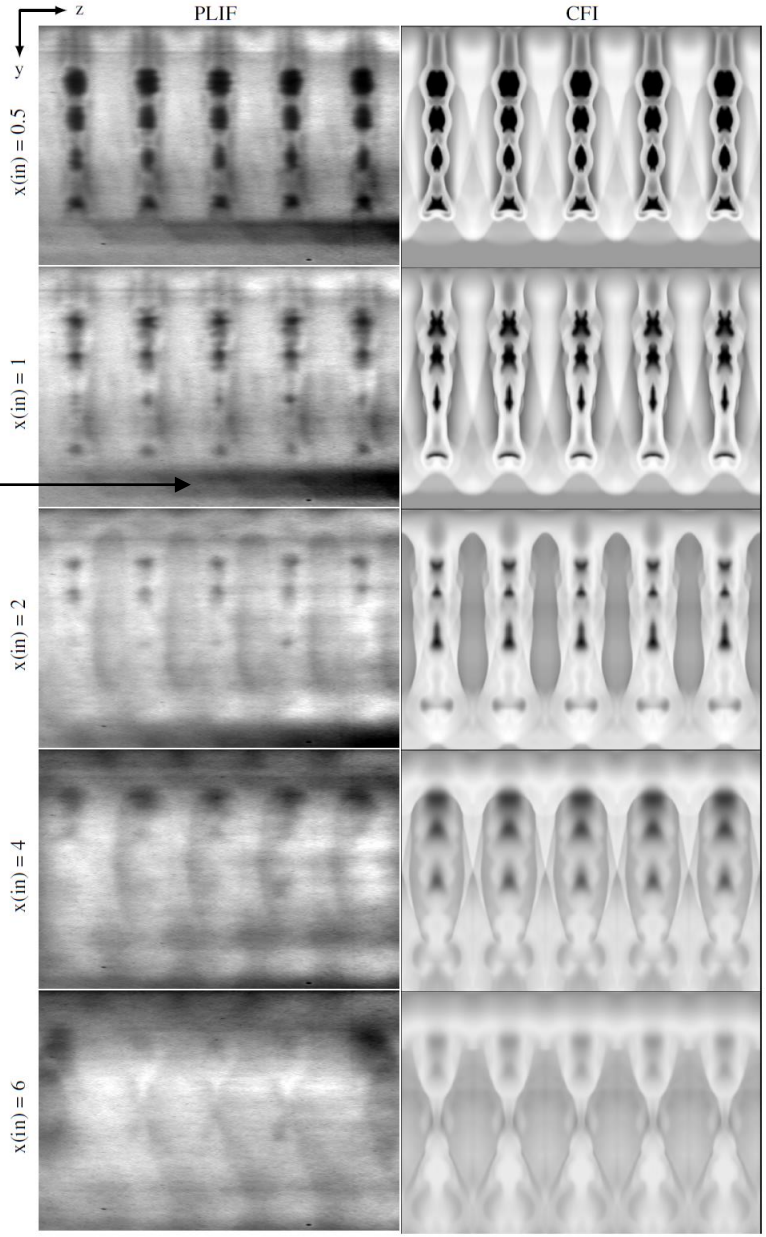

It is difficult to isolate the dominant source of the discrepancies, however, qualitative level of agreement is reasonable

Strut Injector CFD

PLIF oP12(J=14.5) @ x=0.5 in

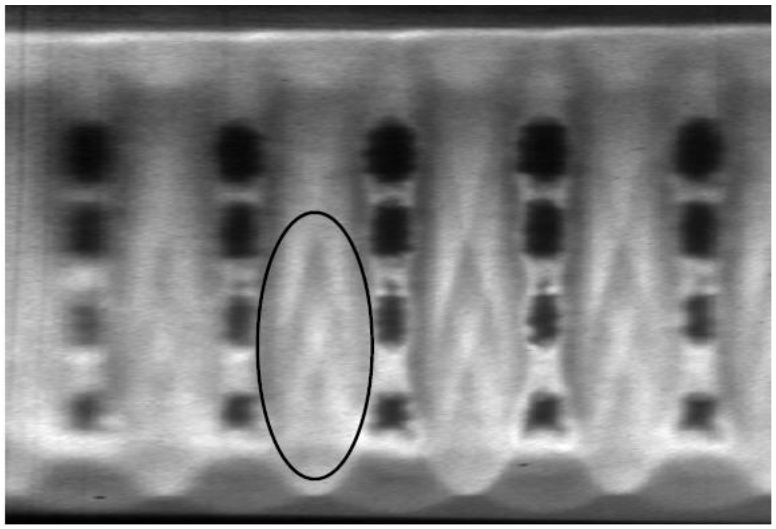

Turbulent Simulation

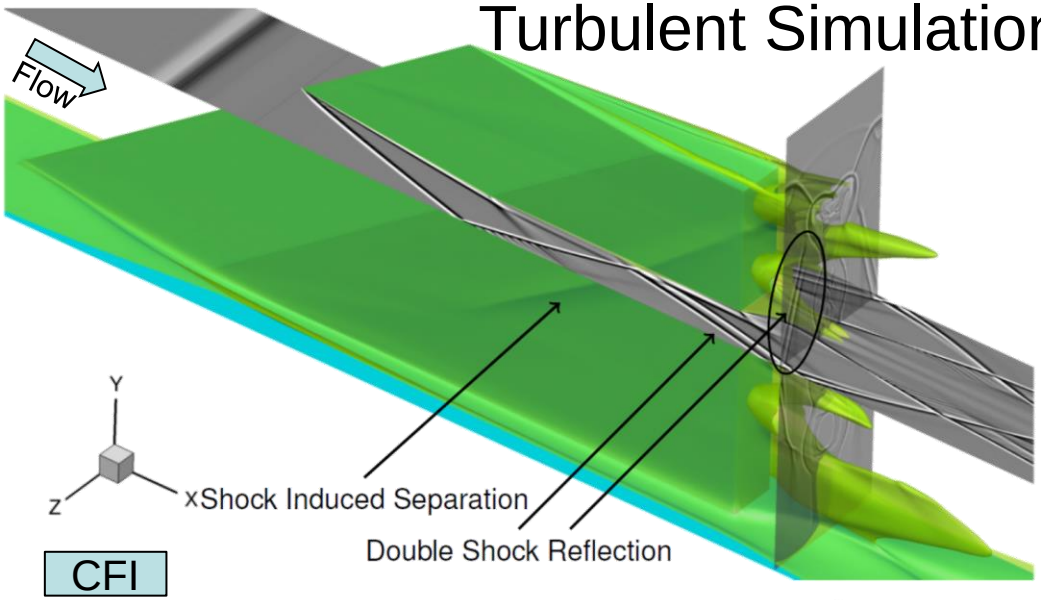

CFI

Turbulent Simulation

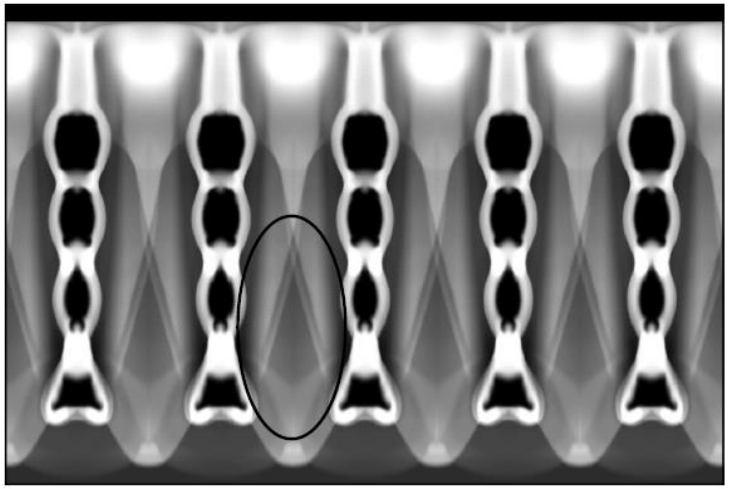

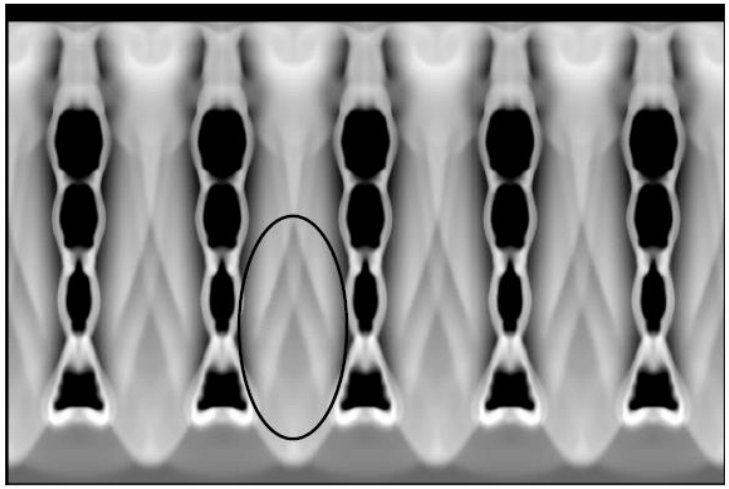

Laminar Simulation

Although mixing is not significantly impacted, to capture downstream shock features a transition model is required

Flushwall Injector Experiments & PLIF Reslicing

- Sequence of PLIF images can also be resliced to produce PLIF images in the other planes to reveal additional flow features … such as extent of turbulence shear-layer fluctuations

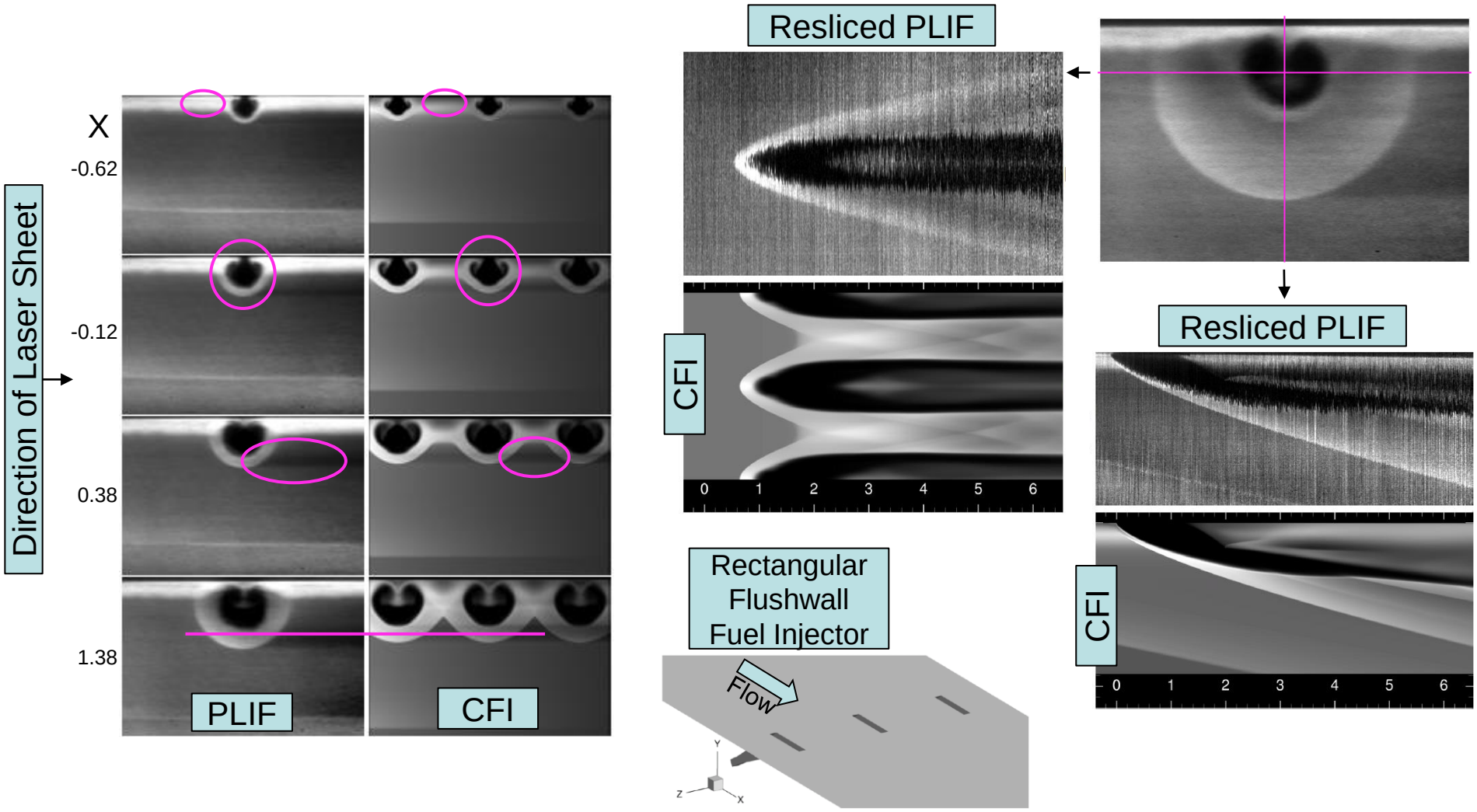

Cross-stream PLIF reslicing qualitatively reveals instantaneous flow features

Flushwall Injector Experiments (cont.)

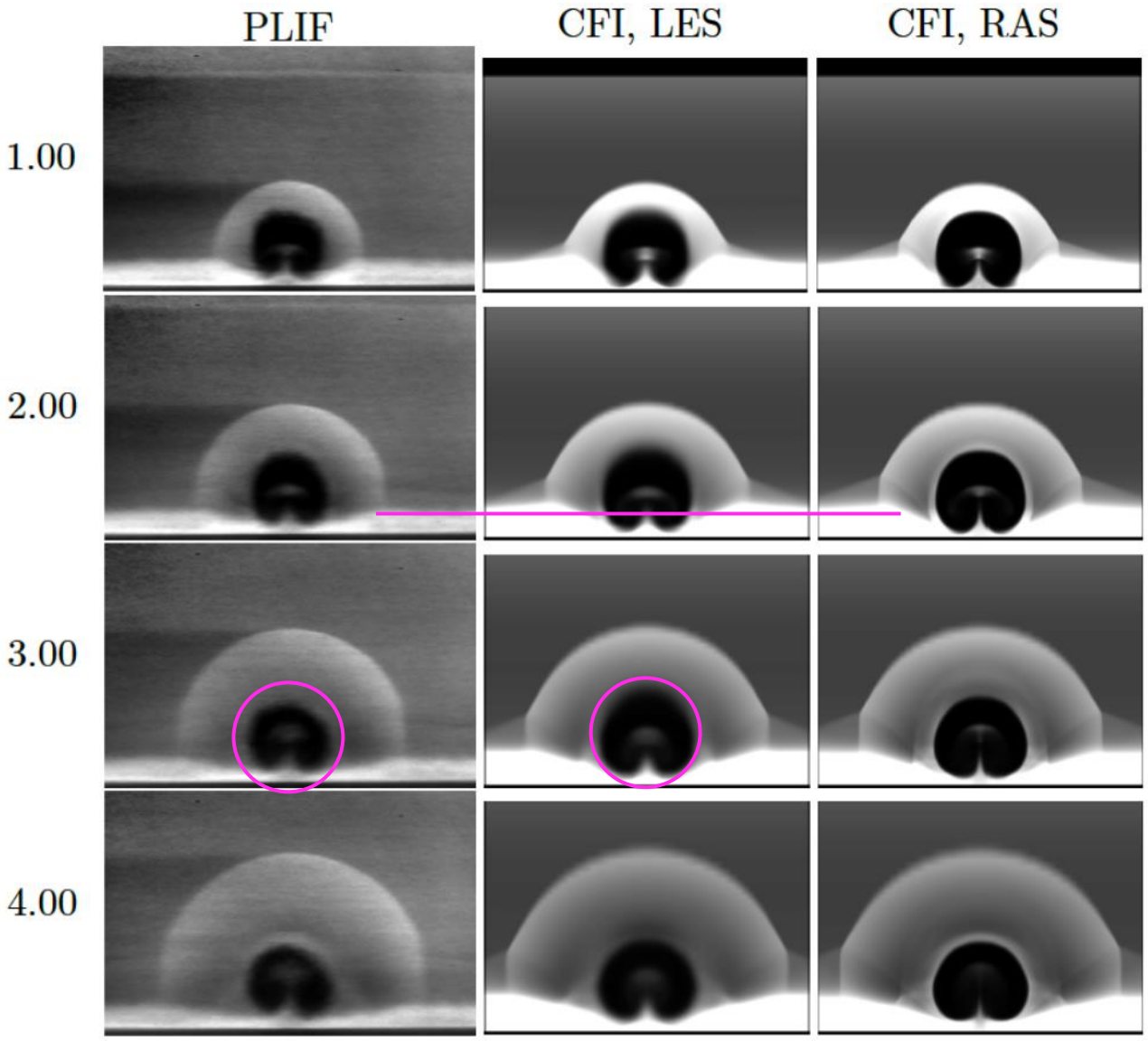

LES captures the nuanced features of the flow more accurately

Sensitivity of the CFI to Sc_t

Menter-BSL
ER=0.75

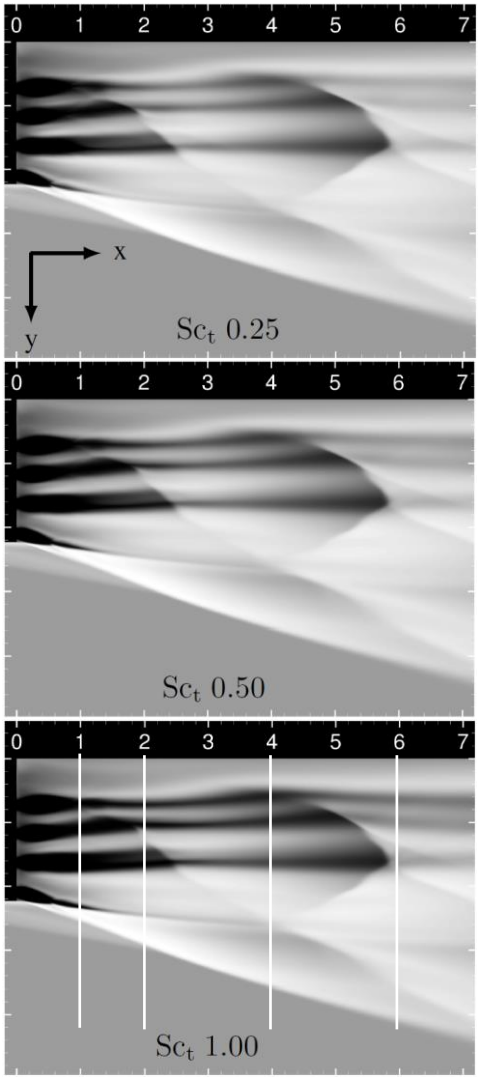

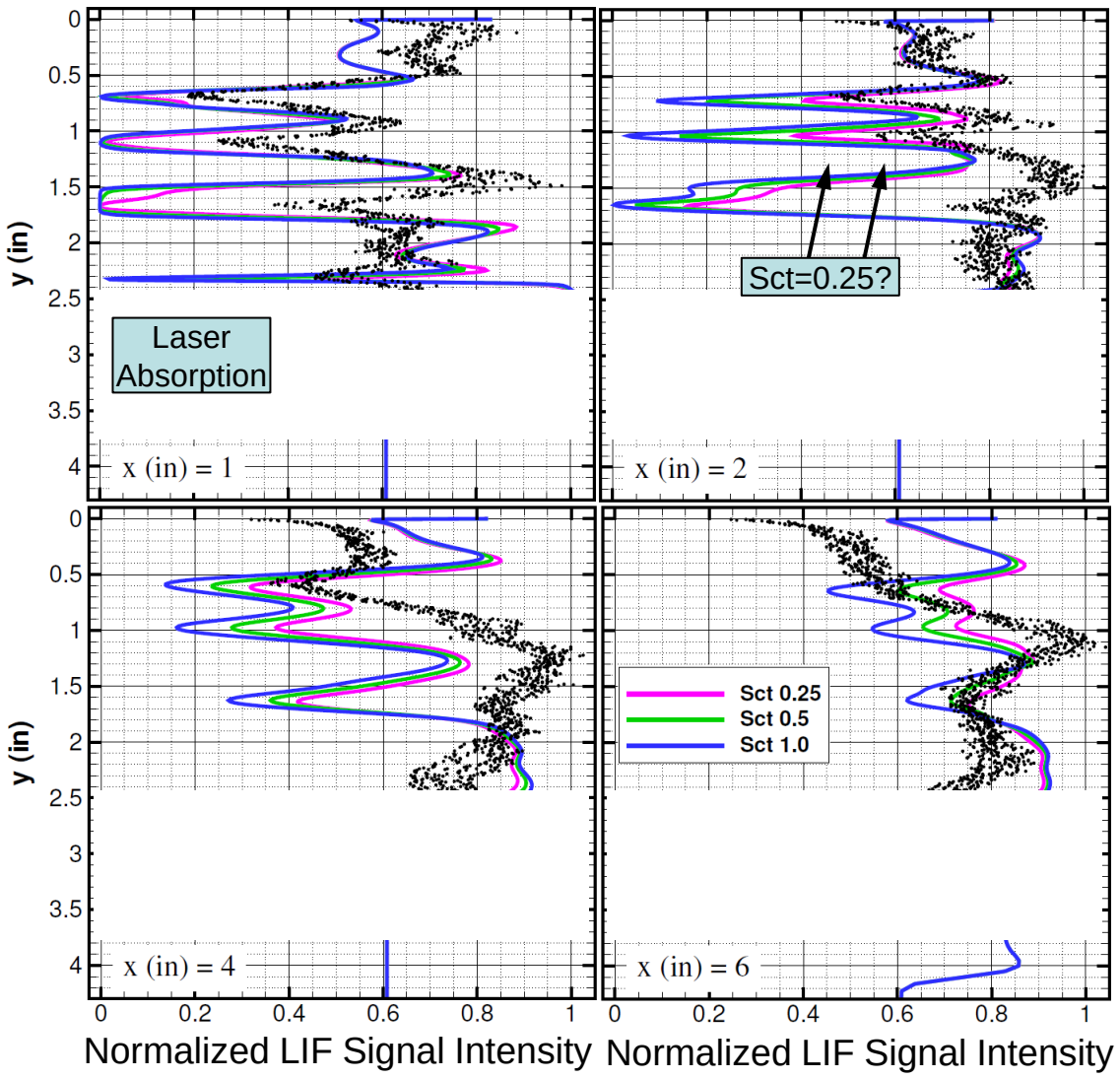

However, for a given turbulence model, it may be possible to use CFI to narrow down the value of the Sc_t. But, need to improve PLIF "quality."

Experiments: Gas Sampling
Hot-Wire-Based Gas Analysis for Binary Mixtures

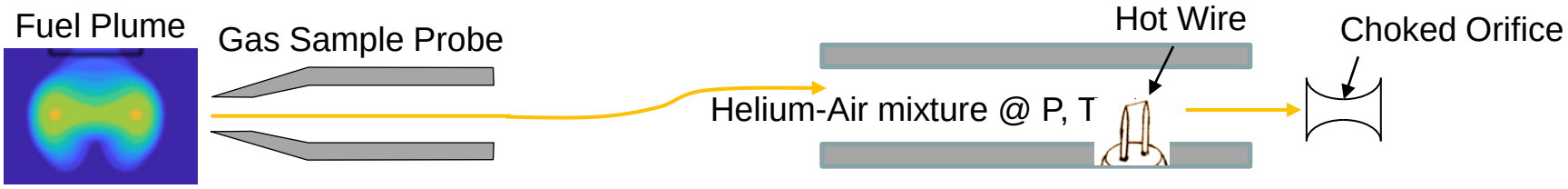

Helium Mole Fraction = func(hotwire voltage, P, T); but T is held constant.

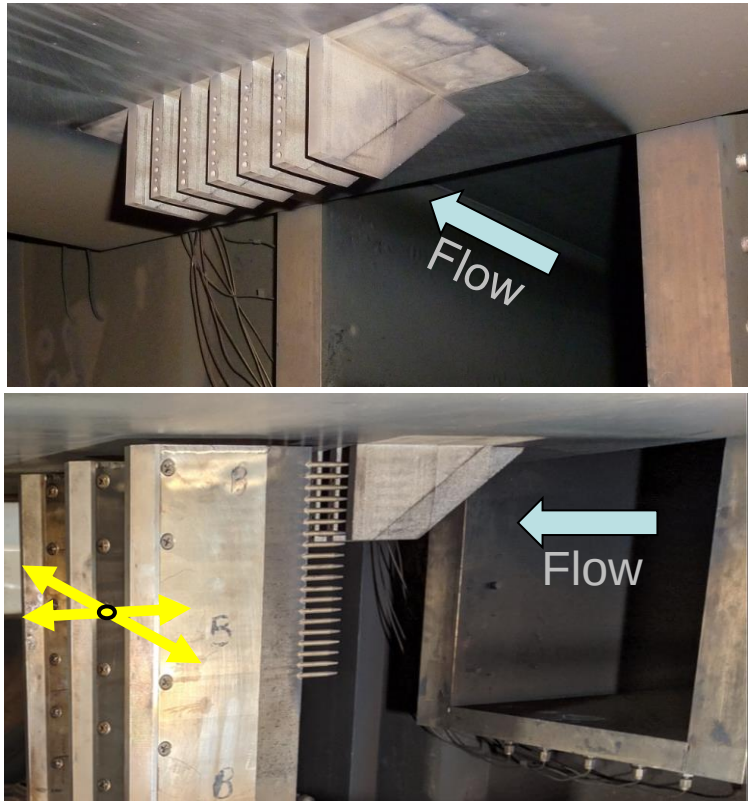

In-stream probes on a traversing rake system are used to survey any cross-stream plane downstream of fuel injector

Available Probes:

- Total temperature probes
- Combined pitot pressure/gas sampling probes

Gas Sampling to Mole Fraction
Example calibration

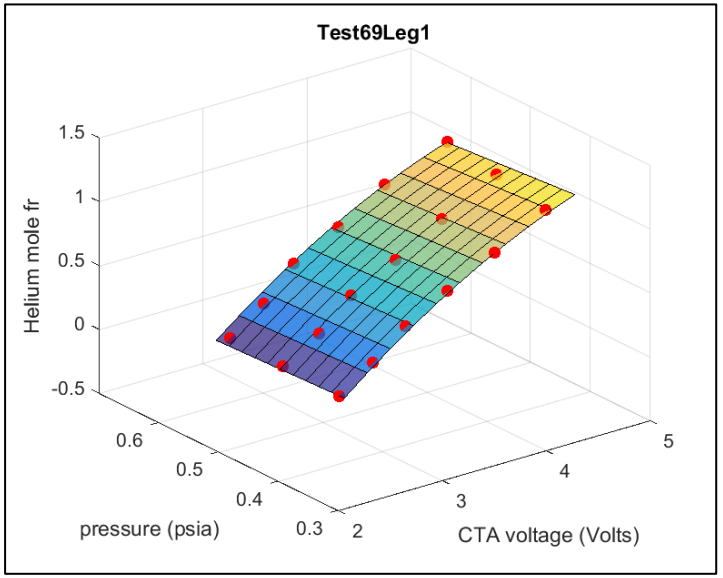

Helium mole fraction is obtained from hot wire voltage via calibration

Experiments: Gas Sampling CFD-Assisted Analysis

- Pretest CFD-assisted analysis of the gas sampling performance at 1/8 x 1/8 inch measurement density

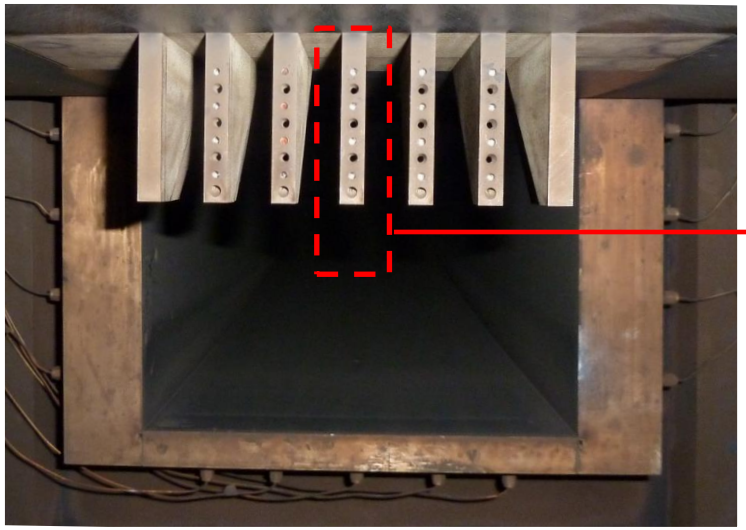

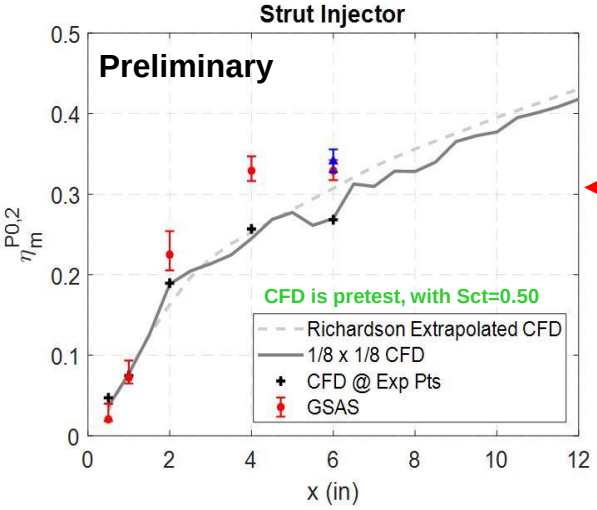

Pretest "simulation" of experimental mixing efficiency

Posttest, the value of the turbulent Schmidt # will be adjusted to achieve match between experiment and CFD

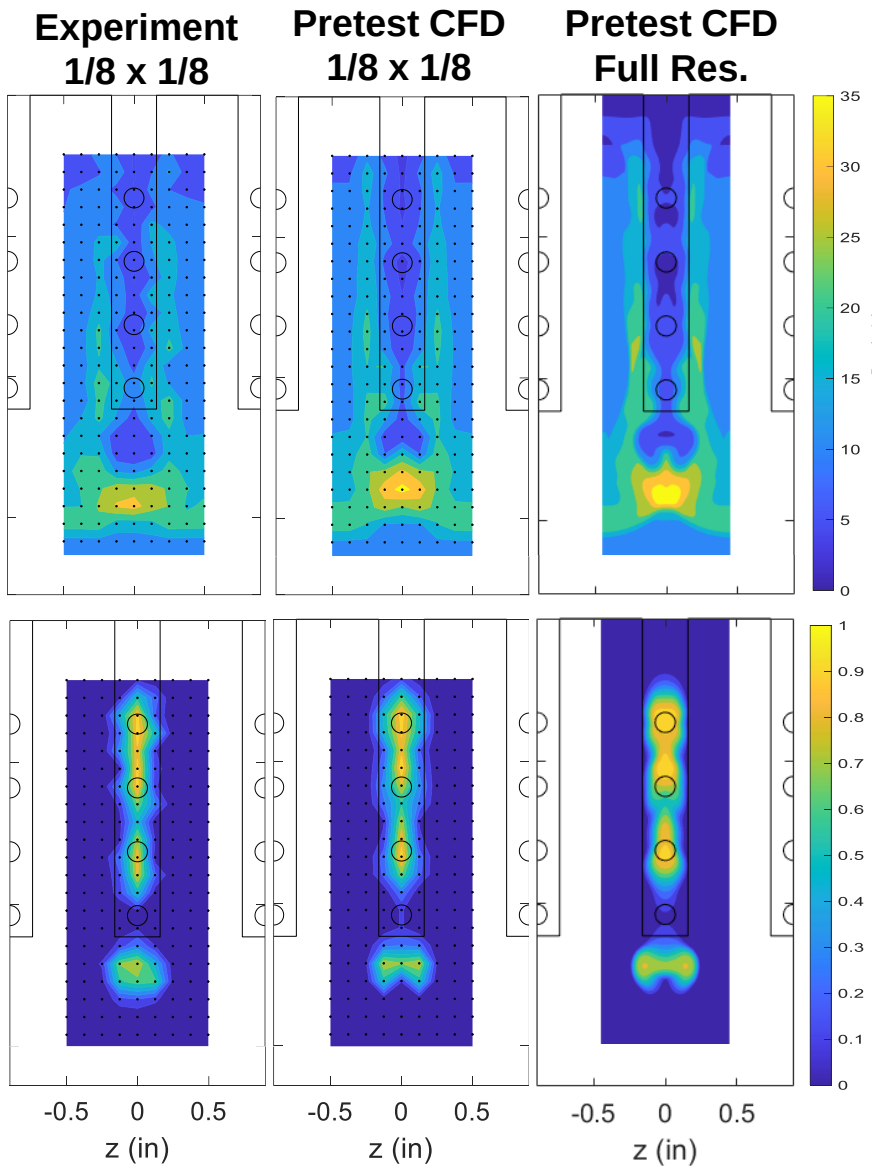

Pretest analysis of the gas sampling methodology indicates sufficient accuracy

Summary and Conclusions

- Recent flight demonstrations of hypersonic vehicles prove their potential for
  - rapid response and strike capability
  - safer and more affordable access-to-space
  - hypersonic point-to-point transport
- However, hypersonic air-breathing flight has been elusive over the last 70 years
- Although our understanding of hypersonic flow phenomena is relatively mature, the multidisciplinary interactions of a large number of competing factors make designing scramjet-powered vehicles very difficult.
- One of the key challenges is the ability to minimize the overall length of a hypersonic vehicle in order to reduce the weight, thermal loads, and drag.
- From a propulsive flowpath perspective, one way to reduce the vehicle length is to reduce the combustor length needed to efficiently inject, mix, and burn the fuel.
- Because the scramjet flow environment is hostile to already limited number of available diagnostics, a tightly coupled experimental-numerical research approach is required to explore new ways to reduce combustor length.
- In addition, further advances are required in numerical methods, turbulence modeling, and computer technologies to enable more rapid and predictive simulations.
- The good news is that there are many exciting problems to solve and …

Although the excitement about hypersonic flight ebbs and flows, it appears we are now in a period of renewed interest

Questions

Summary and Conclusions

- Experiments and CFD are currently being applied at NASA Langley to investigate fuel injection & mixing for high-speed flight applications
  - Experimental diagnostics include NO PLIF flow visualization and gas sampling
- A LIF model was developed, validated, and applied to pretest CFD simulations to obtain computationally-equivalent PLIF flow visualization images (i.e., computation flow imaging or CFI)
- Comparisons of PLIF and CFIs obtained from Reynolds-averaged simulations and large-eddy simulations revealed:
  - strut side-wall boundary layer transition modeling issue
  - mixing plate CFD boundary condition issue
  - that CFIs could “guide” the selection of the turbulent Schmidt number for CFD, however increased PLIF “quality” is needed for actual calibration
  - that although RAS was sufficient, the LES captured nuanced features of the flow more accurately
- Quantitative experimental data obtained via the gas sampling will be used to calibrate the CFD

Reasonable qualitative agreement is observed between the experimental PLIF images and the CFI, thus establishing confidence in the PLIF postprocessing and modeling, and the CFD simulations

Ground Experiments for High Speed Propulsion

Flight

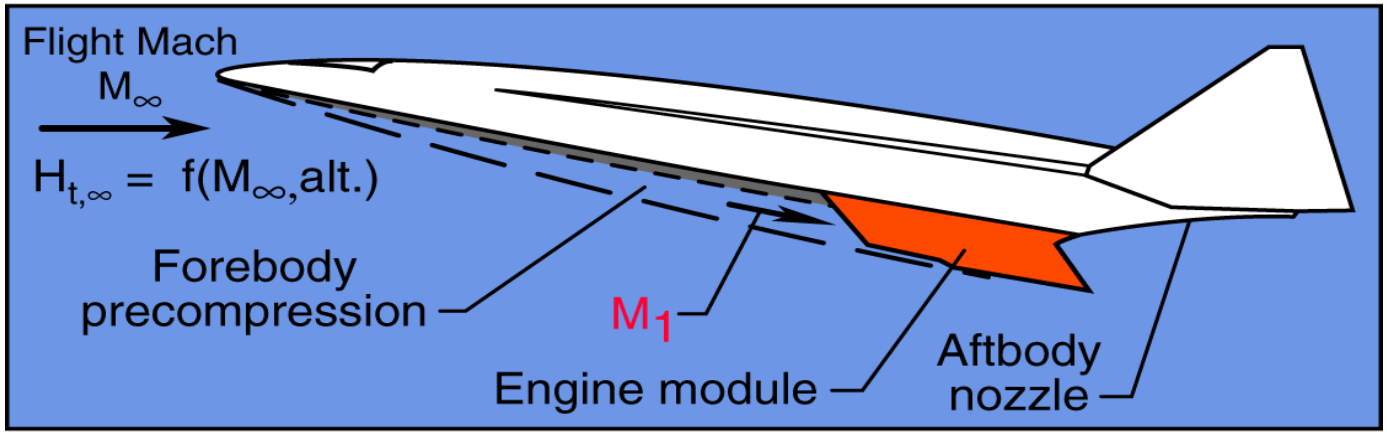

Simulation in ground facility

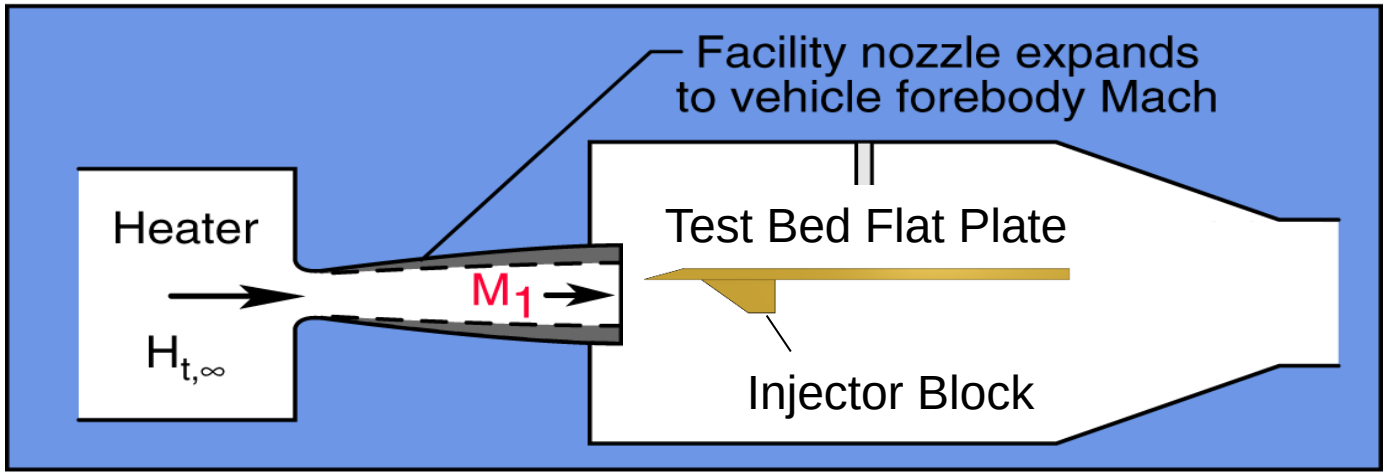

OK2K.1

Primary Experiment Baseline Flow Conditions

Flight:

Alt. (km)	Mach No.	Q (kPa)	P (kPa)	T (K)	$T_0^\dagger$ (K)	P_0 (MPa)
36.6	14.94	71.82	0.4603	249.2	8748.4	1294.7

Inlet with 95%, and 99% isentropic and adiabatic efficiencies

"Combustor" Inflow Conditions:

Alt. (km)	Mach No.	Q (kPa)	P (kPa)	T (K)	$T_0^\dagger$ (K)	P_0 (MPa)	
36.6	6.356	1347.93	50.66	1297.8	8672.8	295.4	
-	6.356	51.12	1.808	112.4	977.8	4.309	AHSTF / Cold

Additional conditions and assumptions:

- Reynolds number is comparable between flight and ground cold flow experiments ~ 0.3e6/in
- Facility air contains NO, which acts as an in situ flow tracer that is imaged using PLIF
- "Combustor" inflow is "undistorted"; experiment is in uniform core of facility nozzle
- Fuel injection:
  - helium (simulating hydrogen)
  - injection Mach≈3, underexpanded
- RAS simulations were conducted pretest using VULCAN-CFD
  - numerical and physical model selections and boundary conditions were based on SME experience and best practices for similar flow configurations
  - using Menter Baseline turbulence model

LIF Modeling Evaluation Criteria

The theoretical models are evaluated based on the following criteria:

1. Are lines in the right place as compared to the experiment? (Gas Cell)
2. Are the line intensities reasonably predicted? (Gas Cell)
3. Are the line relative-intensity changes with temperature and pressure predicted? (Injector Experiment)
4. Are the line widths reasonably predicted? (Gas Cell)
5. Can discrepancies be explained based on our understanding of the experiment and models?

What level of comparison is good enough?

- For CFI to PLIF comparisons, we need **1** because the laser is tuned to a single LIF line, and we need **3** because signal intensity is normalized for both CFI and PLIF.

Introduction and Motivation

- Schlieren is a common line-of-sight flow visualization of the density gradients in the flow that can often hide interesting flow features
- Here, schlieren is used to visualize flow from fuel injector … presence of fuel is not obvious … even for “planar” schlieren, but PLIF of the same flow …

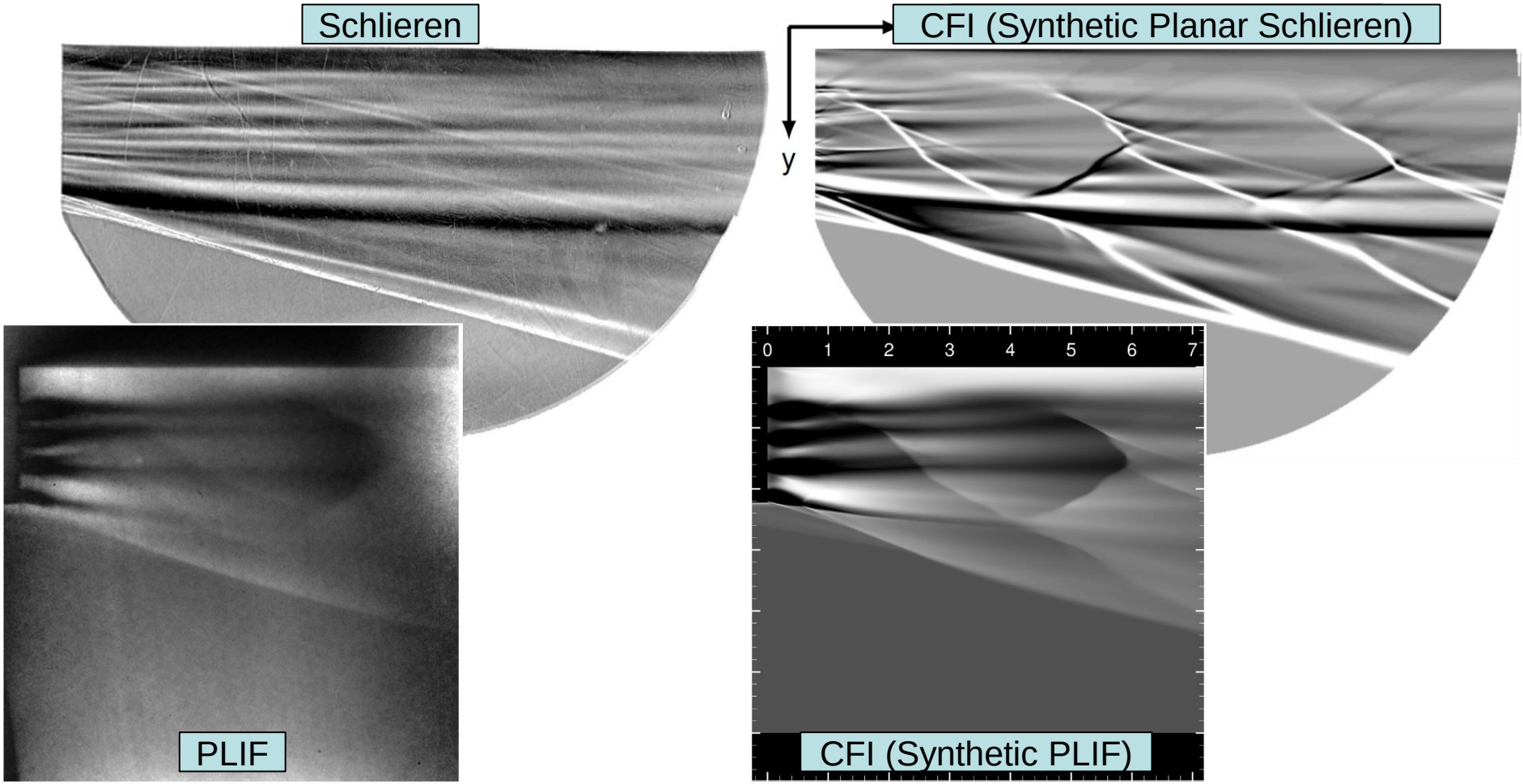

NO PLIF Laser System

- Laser system:
  - Injection seeded Spectra Physics Pro-230 Nd:YAG laser pumps a Sirah Cobra Stretch dye laser and Sirah Frequency Conversion Unit (FCU)
  - Output (near 226 nm) tuned to excite a variety of weak spectral lines of NO to minimize absorption
- High-efficiency filters transmit the LIF signal while rejecting the laser scatter
- LIF is imaged onto a CCD with 16-bits of resolution
- Nikon UV lens is used for the primary experiment
- Halle UV lens is used for the secondary experiment
- Scheimpflug mount is used for the primary experiment to improve focus
- Camera magnifications and perspective in the primary experiment are taken into account by imaging a “dotcard”
- Images are obtained at a rate of 10 Hz

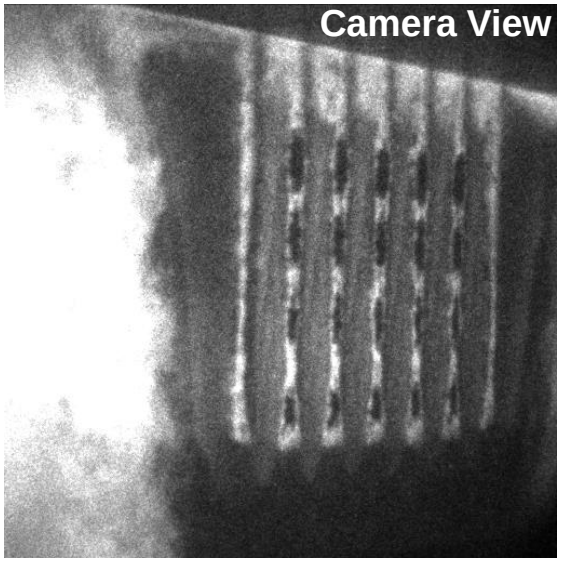

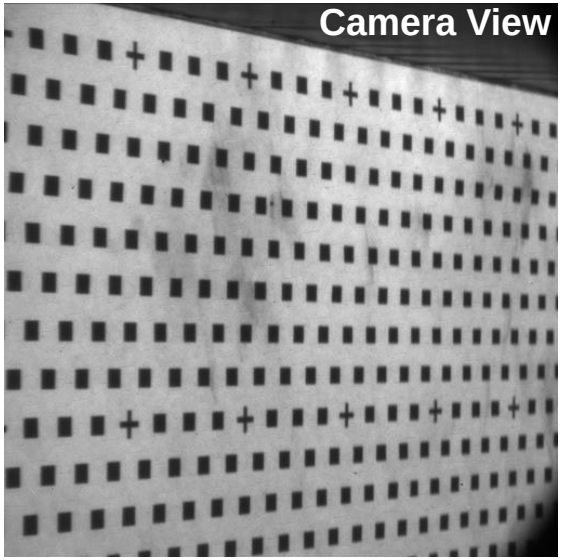

PLIF Image Postprocessing: Unwarping

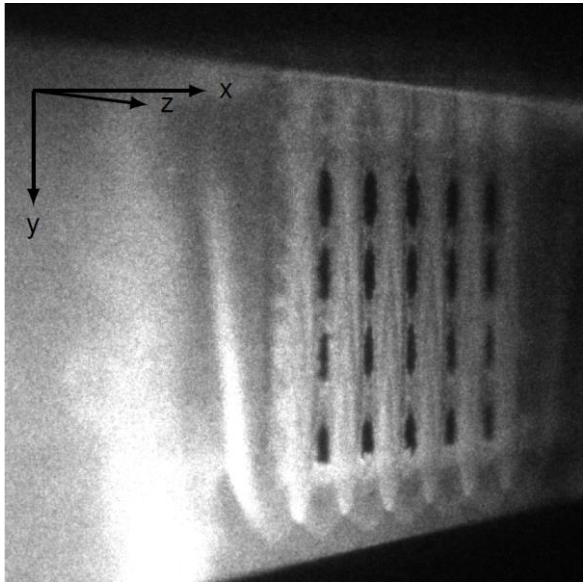

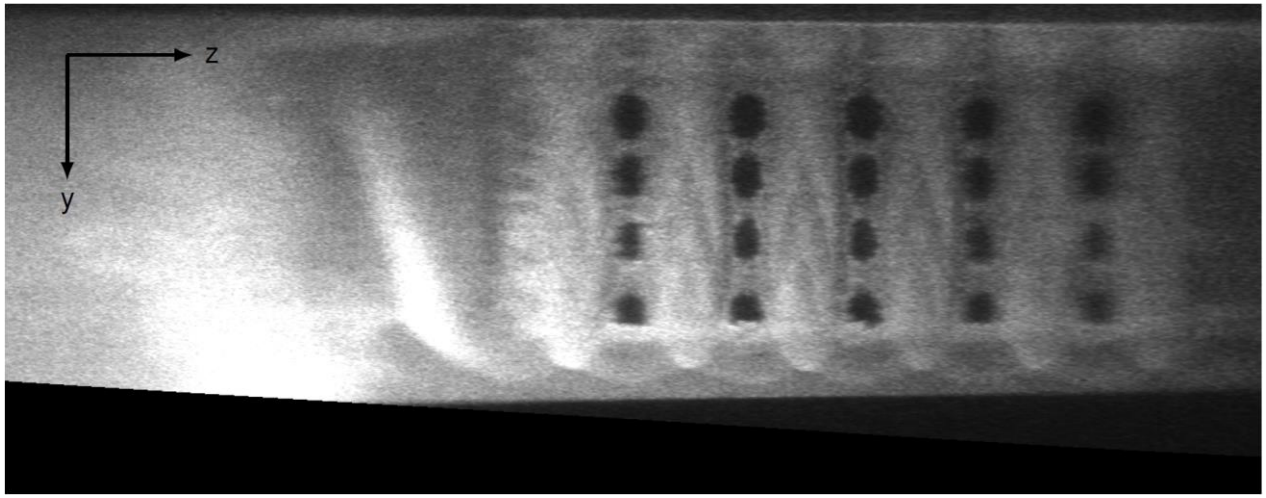

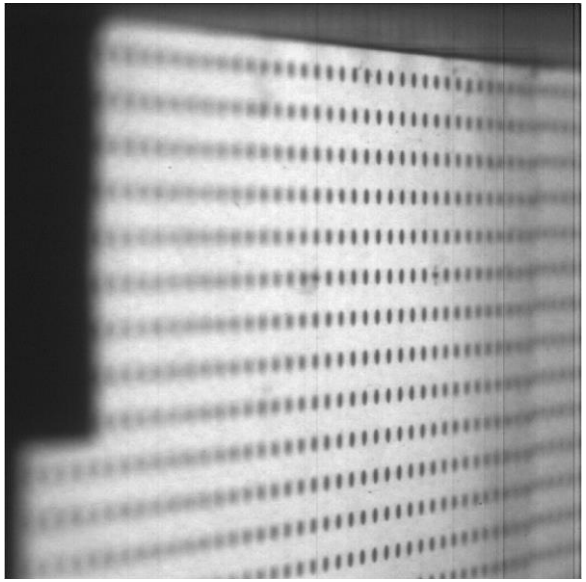

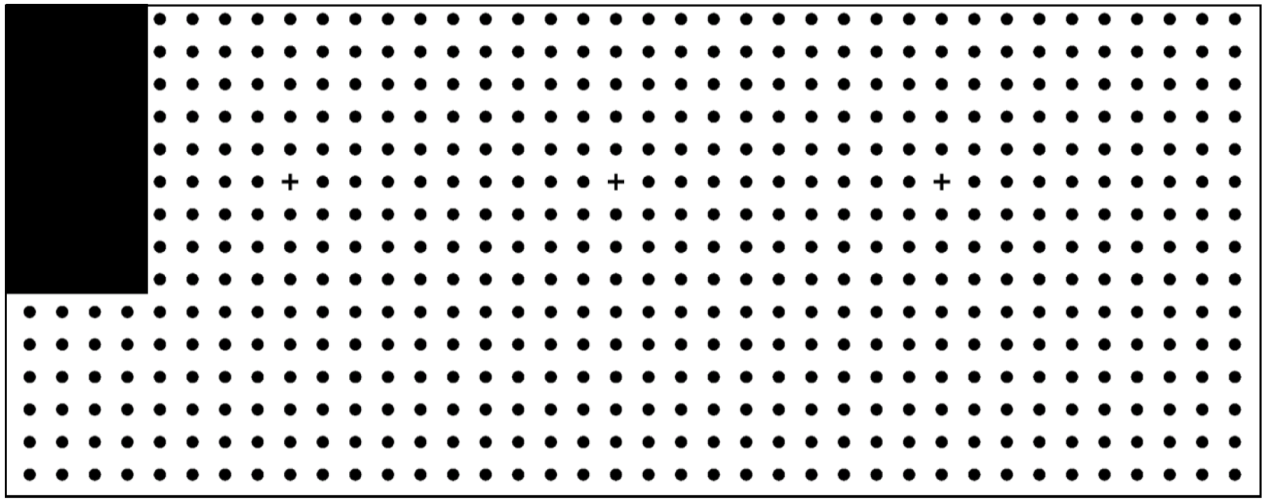

PLIF Image Postprocessing: Absorption (Partial)

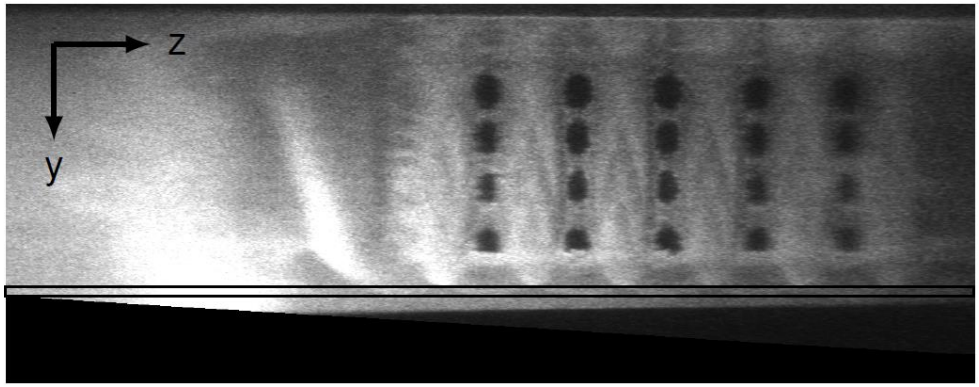

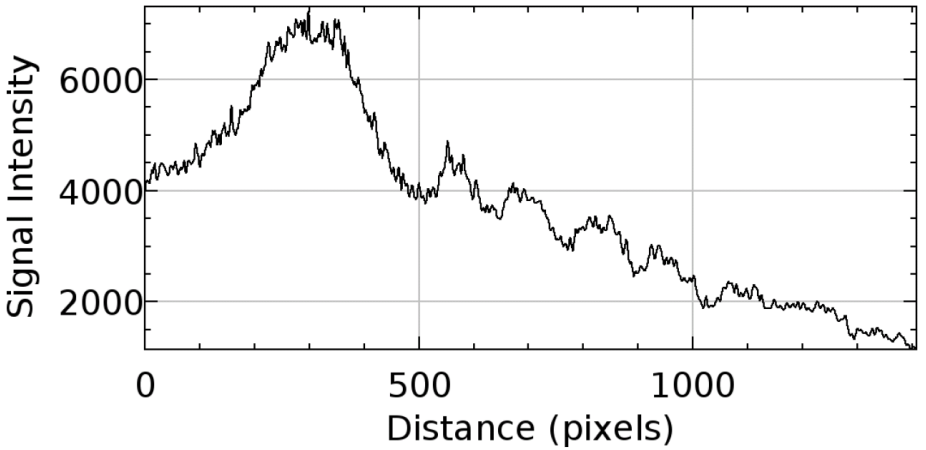

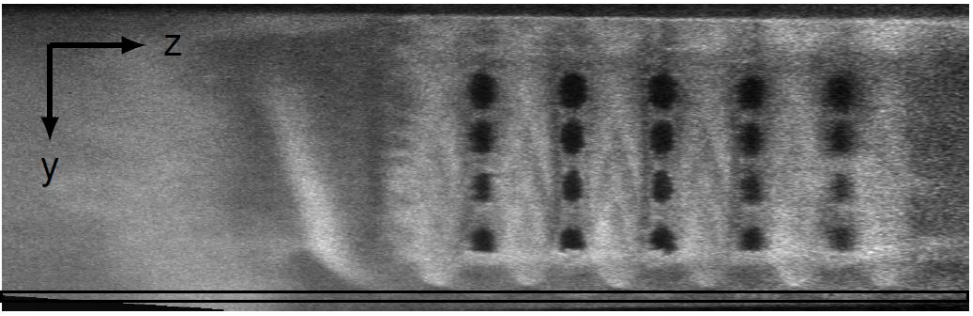

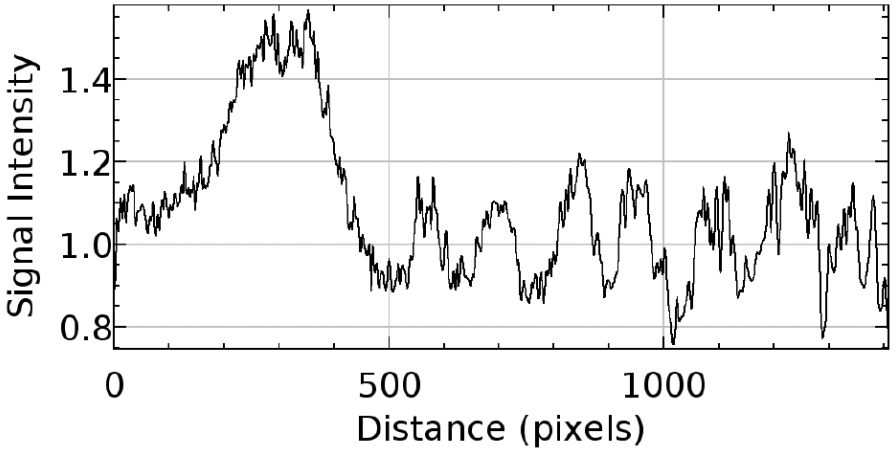

3D Reconstruction of Cross-Stream PLIF

$$SF(pixels/frame) = \frac{STR(in/s)}{FR(frame/s)} \times TDR(pixels/in),$$

Reconstructed Dimension Scale Factor

Target Dotcard Resolution: 146.7 (pixels/in)

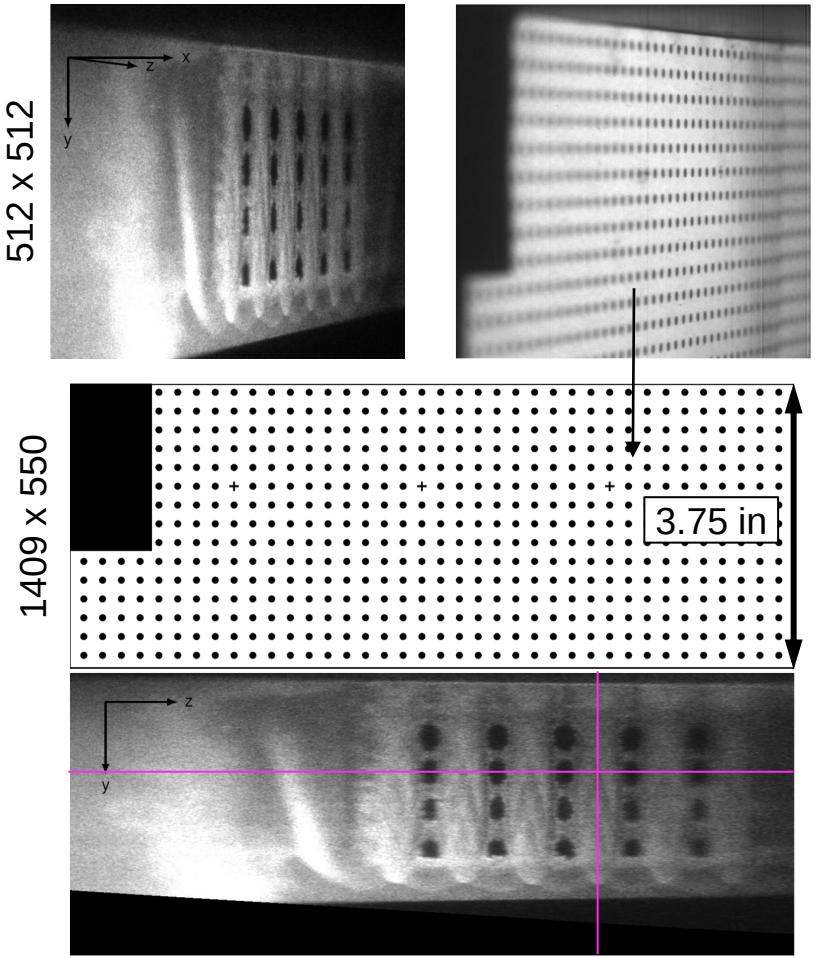

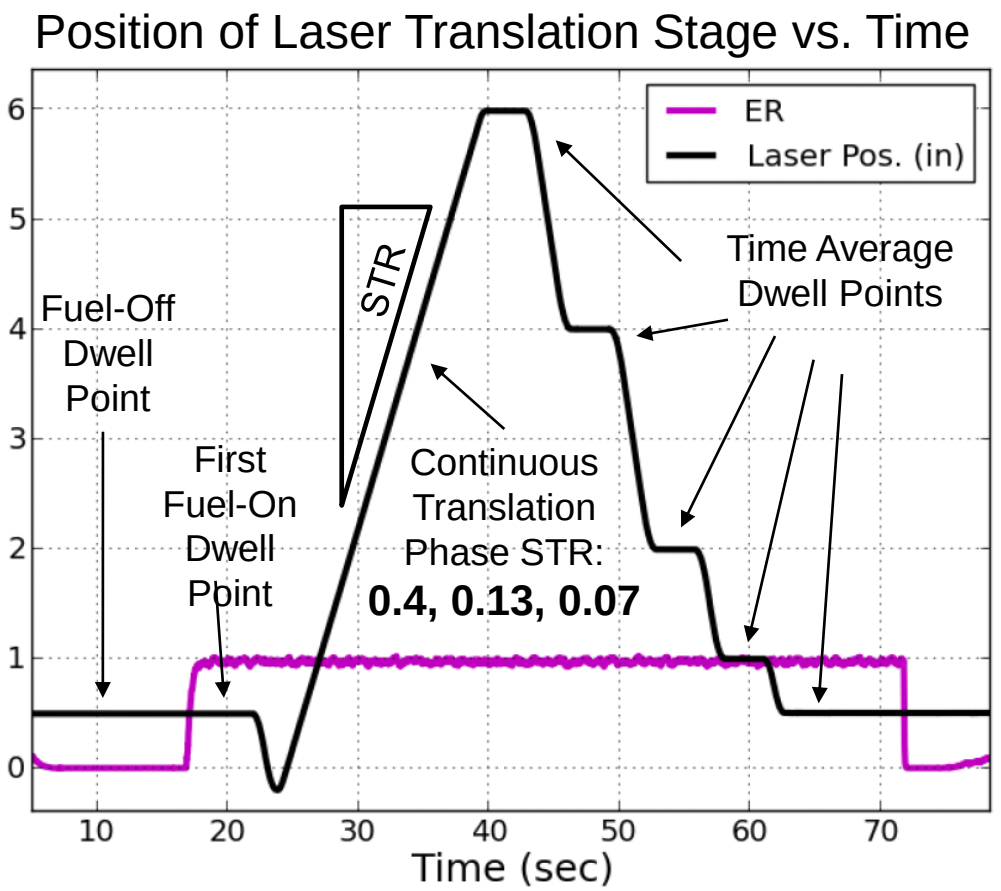

Scanned Segments of the NO LIF Spectrum

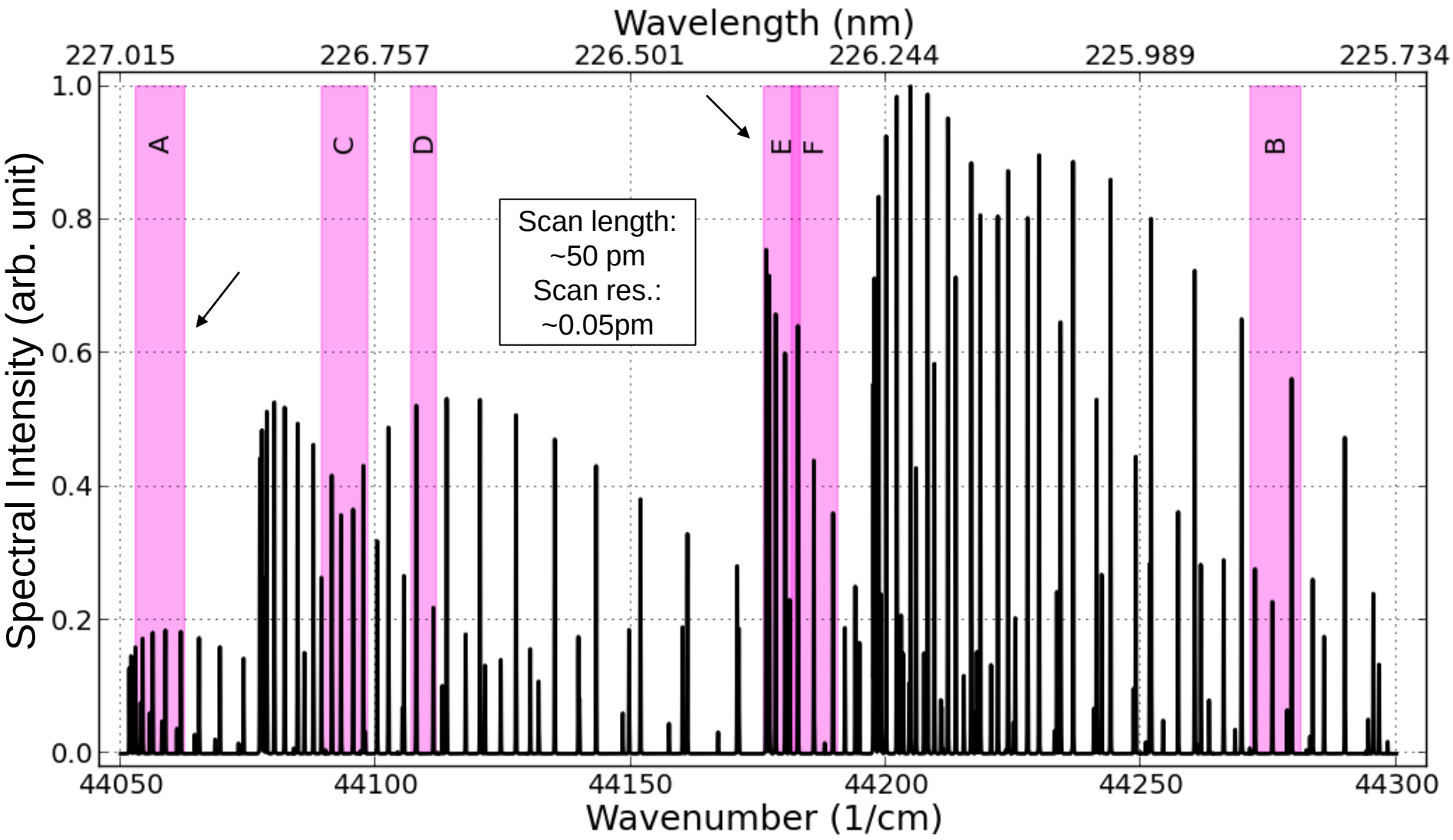

Selected segments contain rotational quantum numbers primarily in the range of 2.5-16.5 that exhibit large Boltzmann fractions for temperatures up to about 1000 K

Gas Cell Spectra: Scan E (Previous Results)

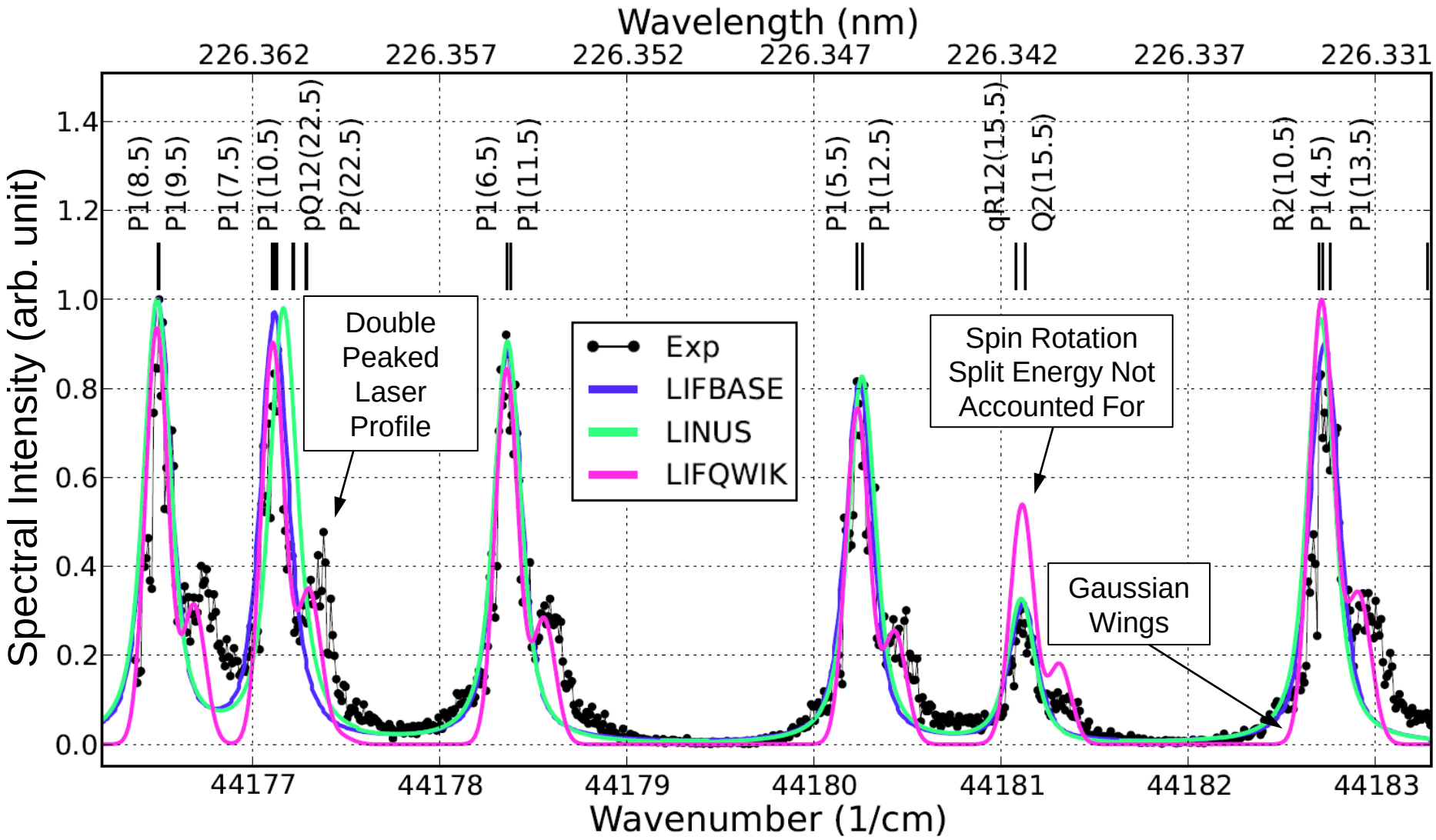

Lorenzian laser profile offers a better match with data

Gas Cell Spectra: Scan E (Current Model)

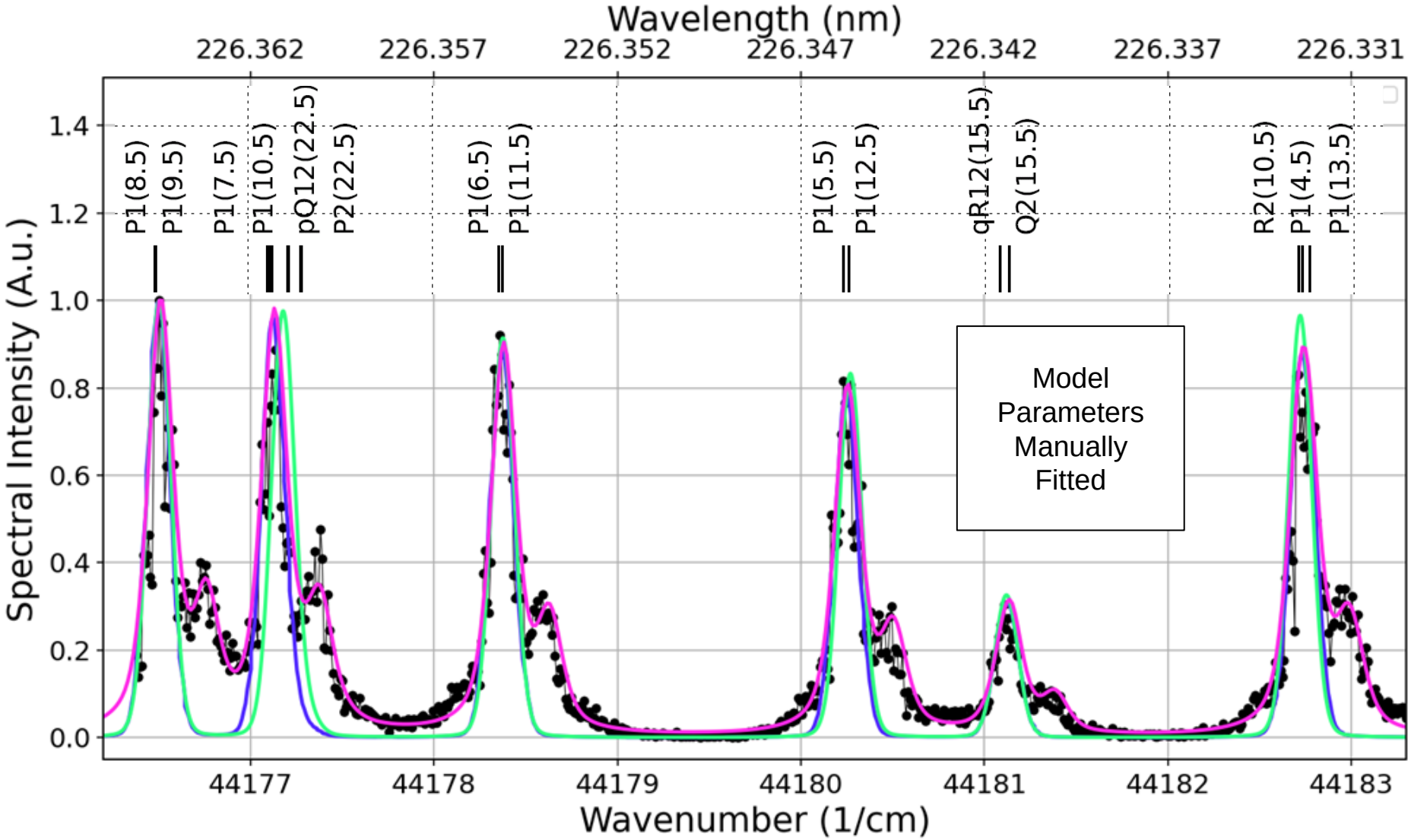

Voigt spectral overlap profile offers a better match with data

Gas Cell Spectra: Scan E (Current Model)

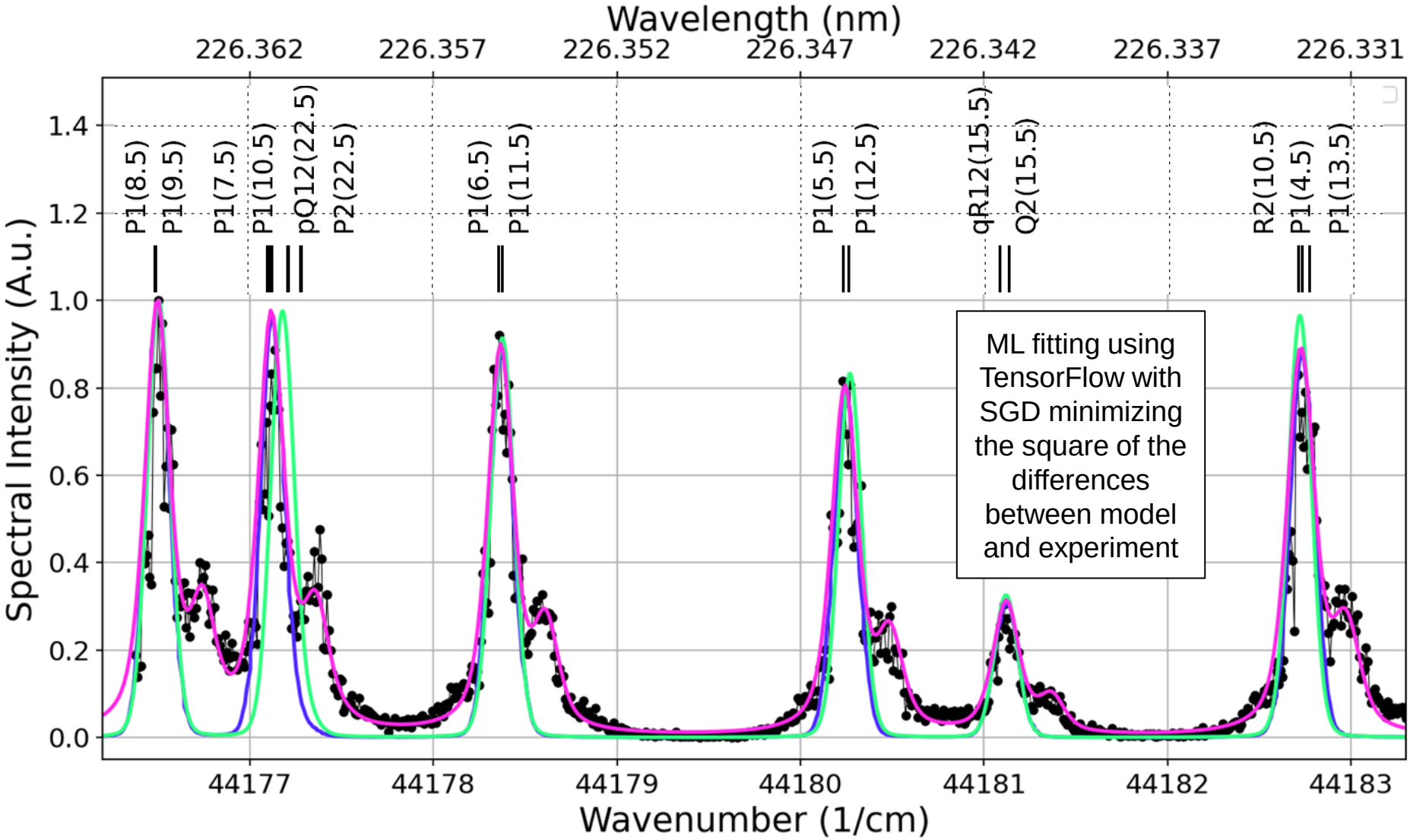

Automated parameter fitting reproduces “human eye” fitting

Mixing Experiment Spectra: Test Cabin Temperature Estimate (Scan A)

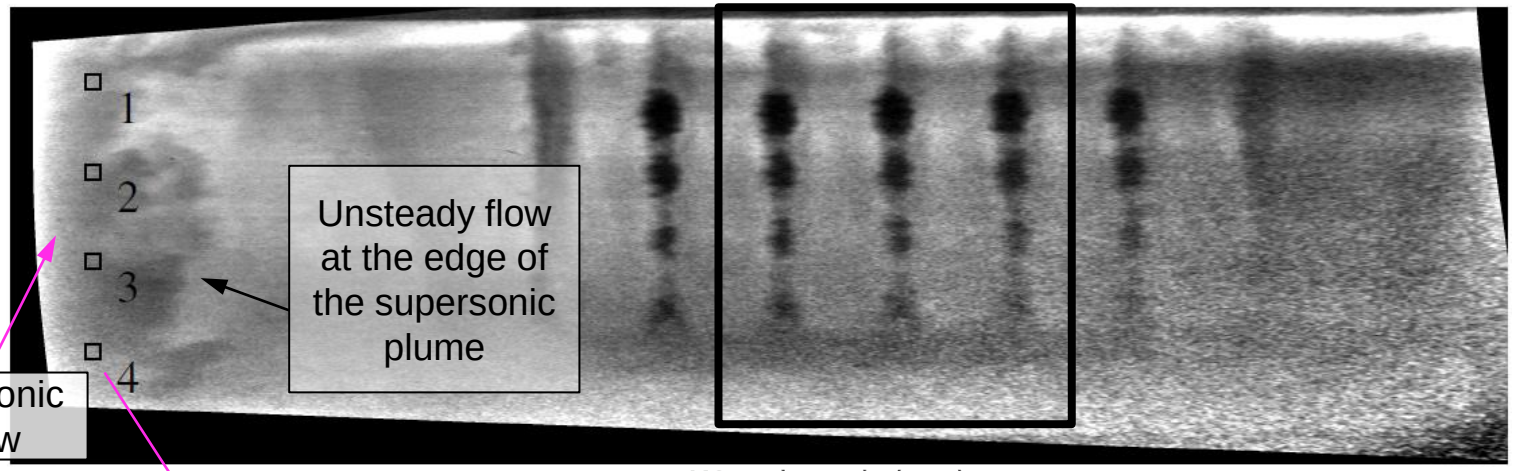

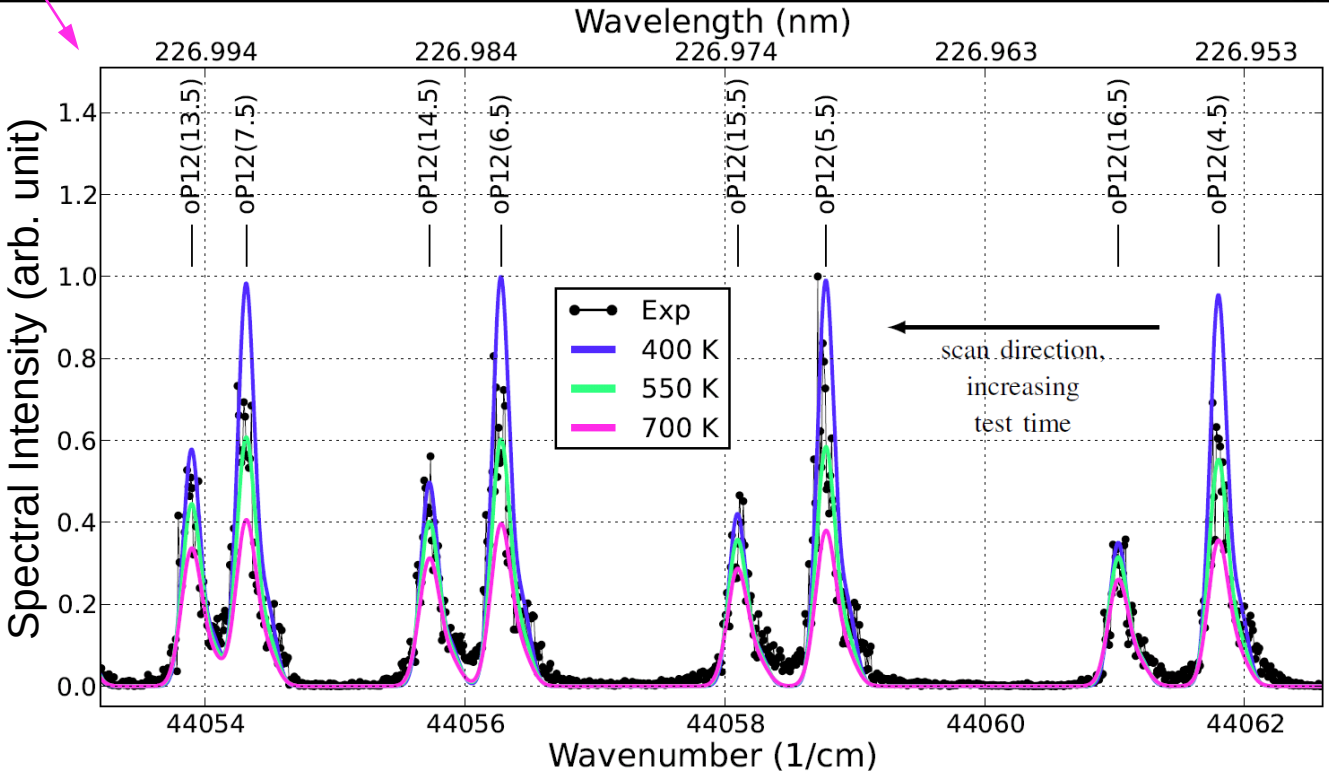

Doppler Shift in PLIF and Modeled in CFI (Scan A)

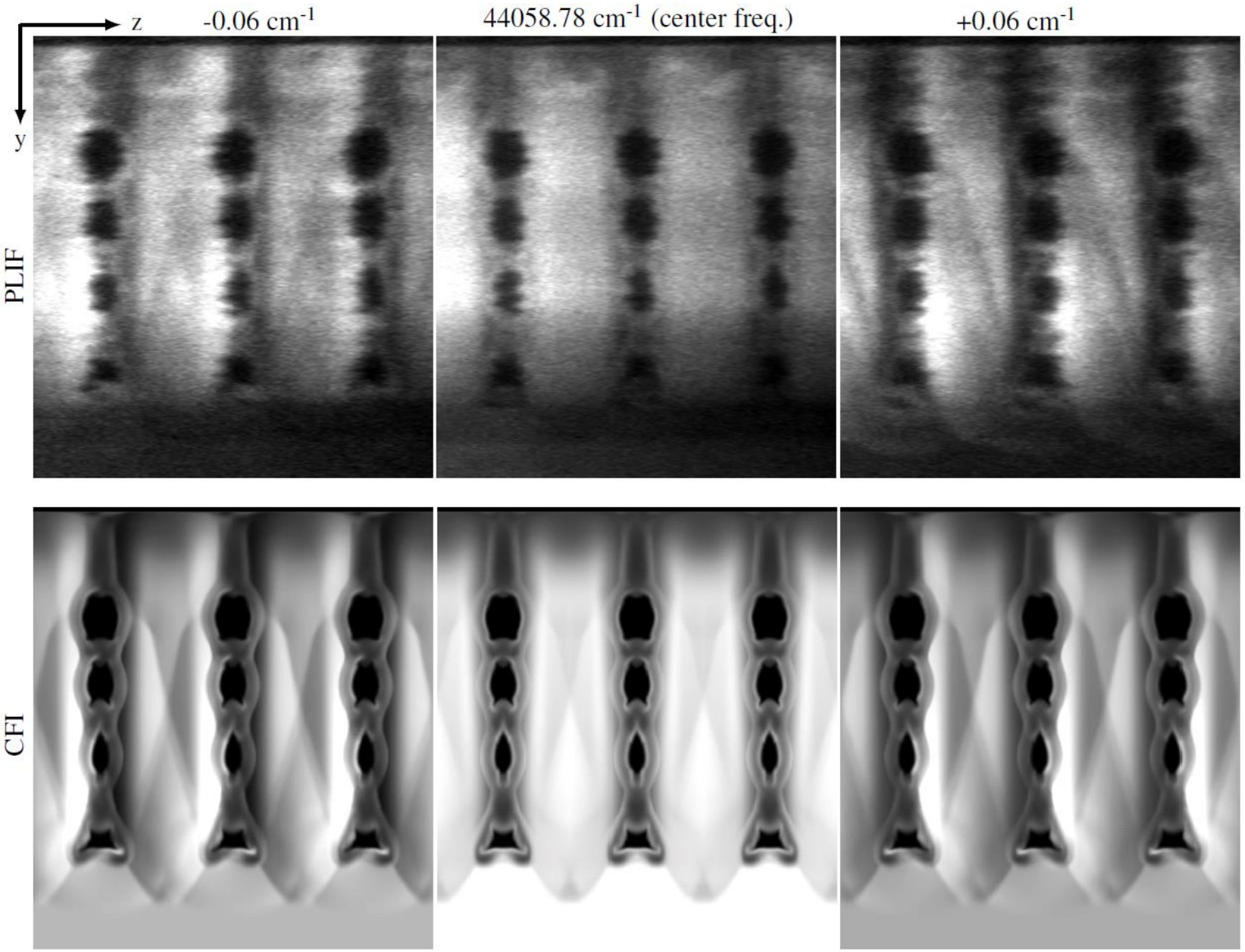

oP12(5.5)

Flushwall Injector BL Attenuation in CFI

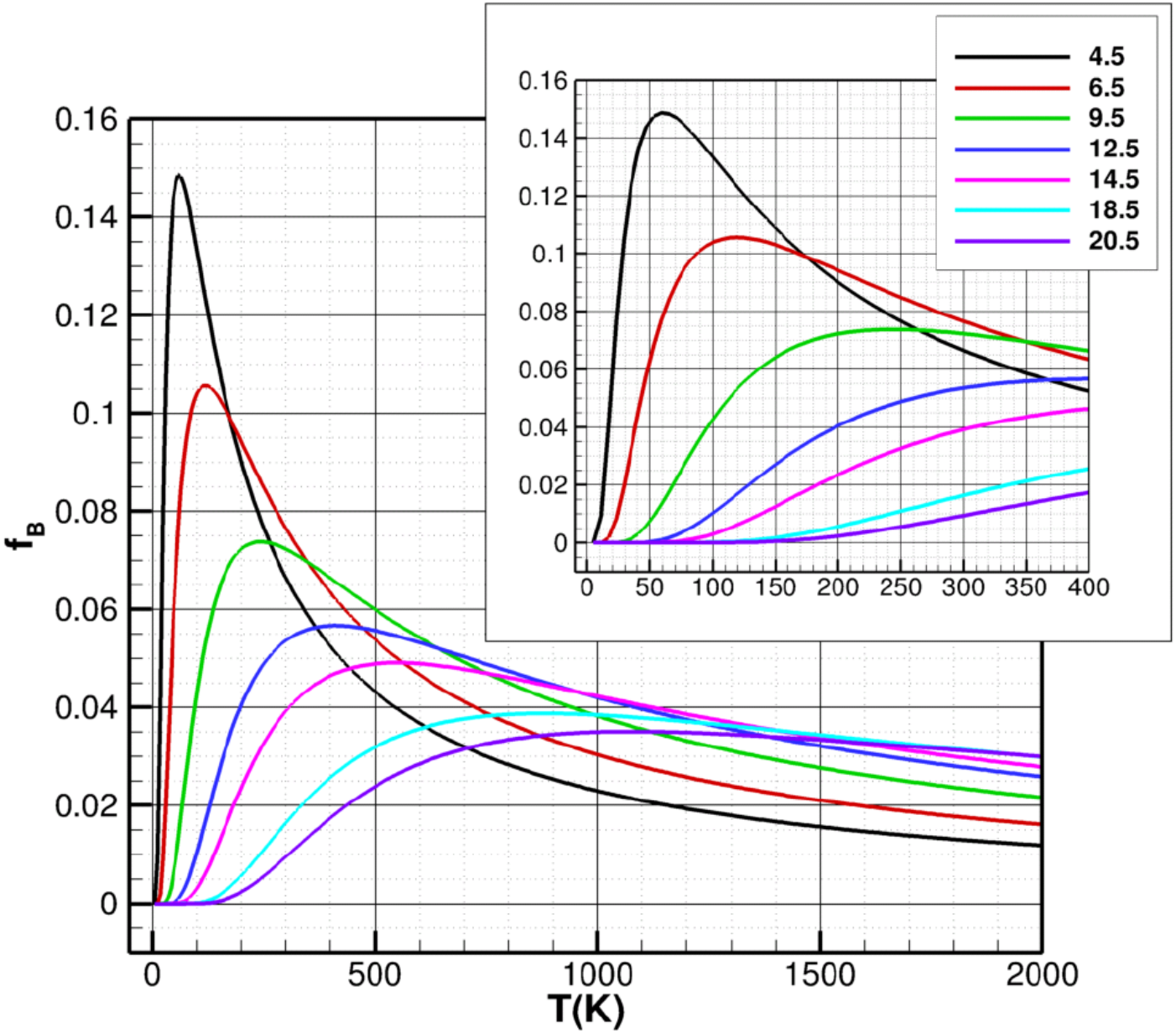

Numerical Simulations

All numerical simulations were performed using the Viscous Upwind aLgorithm for Complex flow ANalysis (VULCAN-CFD) code

- **Reynolds-averaged simulations (RAS) were performed prior to ground testing.**
- The advective terms were computed using a MUSCL scheme with the Low-Dissipation Flux-Split Scheme (LDFSS).
- The governing equations were integrated using an implicit diagonalized approximate factorization (DAF) method.

- Baseline blended $k-\omega/k-\varepsilon$ turbulent model of Menter was used for all calculations.
- Reynolds heat and species mass fluxes were modeled using a gradient diffusion model with turbulent Prandtl and Schmidt numbers of 0.9 and 0.5.
- Wilcox wall matching functions were also used, where appropriate.
- The convergence was monitored via the L_2-norm of the steady-state equation-set residual.
- All simulations were converged until the total integrated mass flow rate and the total integrated heat flux on the walls remained constant and the residual decreased by 4-5 orders of magnitude.

Numerical and physical model selections were based on SME experience and best practices for RAS of similar flow configurations

Experiments: Gas Sampling CFD Assisted Analysis

Enhanced Injection and Mixing Project

Use of experimental data for CFD calibration

The streamwise profile of a global mixing metric, such as 1-D mixing efficiency, is valuable for anchoring or "calibrating" the CFD. But not enough information is available from the experiments to calculate the mixing efficiency:

$$\eta_m = \frac{\int \alpha_R \rho u dA}{\int \alpha \rho u dA} \qquad \alpha_R = \begin{cases} \alpha, & \alpha \le \alpha_{st} \\ \dfrac{\alpha_{st}}{1-\alpha_{st}}(1-\alpha), & \alpha > \alpha_{st} \end{cases}$$

However, an alternate mixing metric, obtained by substituting pitot pressure for mass flux in the above equation, has been shown to be nearly identical to the true mixing efficiency.

Actual mixing efficiency and pitot pressure-based mixing efficiency profiles

Calculated from pretest CFD of baseline strut, ramp and flushwall injectors

(Ground et al. AIAA-2020-3106)

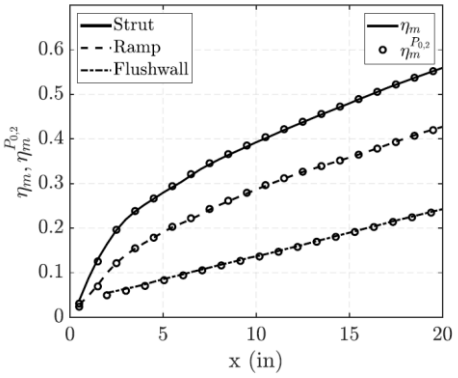

This pitot pressure-based mixing efficiency can be calculated from both the experiments and the CFD.

In post-test CFD, the value of the turbulent Schmidt # will be adjusted to achieve the best match of the pitot pressure-based mixing efficiency profile.

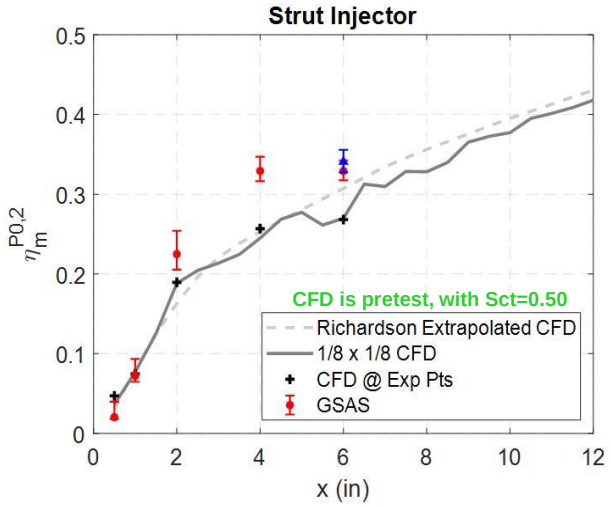

Predicted sensitivity to Sct

Baseline Strut at high Tt ground test cond., Lsep=0.9" ER=0.75 for 3" high IFA

(Drozda et al. AIAA-2019-0128)

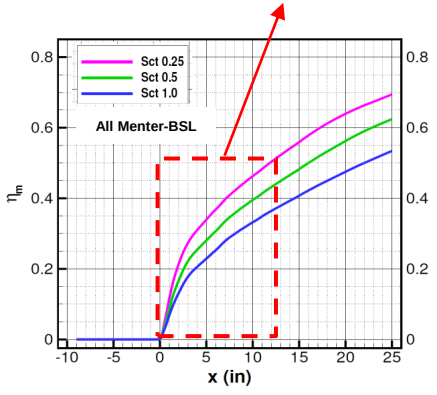

Coupling Between Experiment and CFD

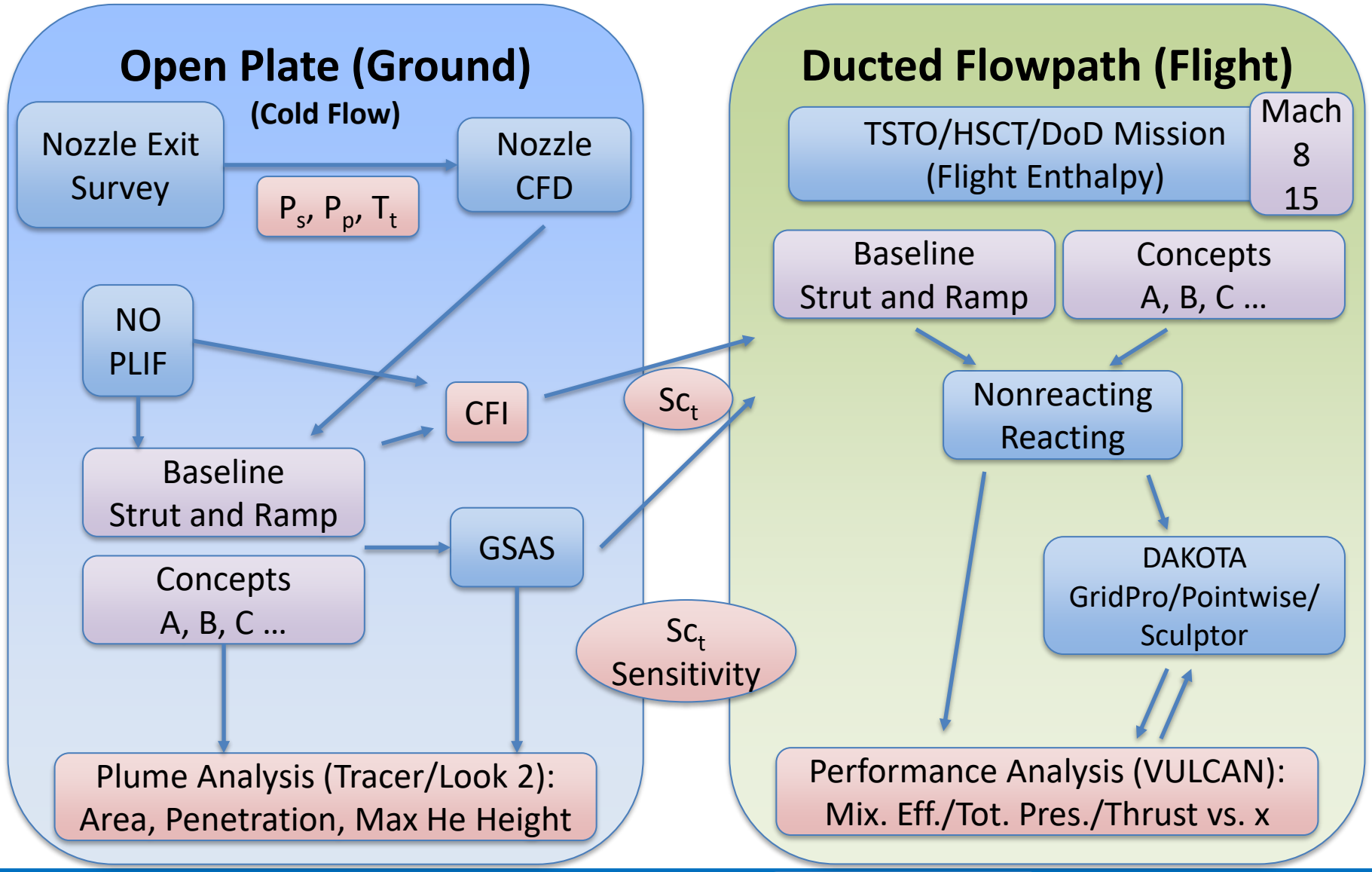

Data Gathering Technique/Concept | Cases Considered | Data Analyzed